Impact of α-hydrazino acids embedded in short fluorescent peptides on peptide interaction with DNA and RNA

Josipa Sućˇ, Lidija-Marija Tumir, Ljubica Glavaš-Obrovac, Marijana Jukić, Ivo Piantanida and Ivanka Jerić

SUPPORTING INFORMATION

Content

Compound **1**

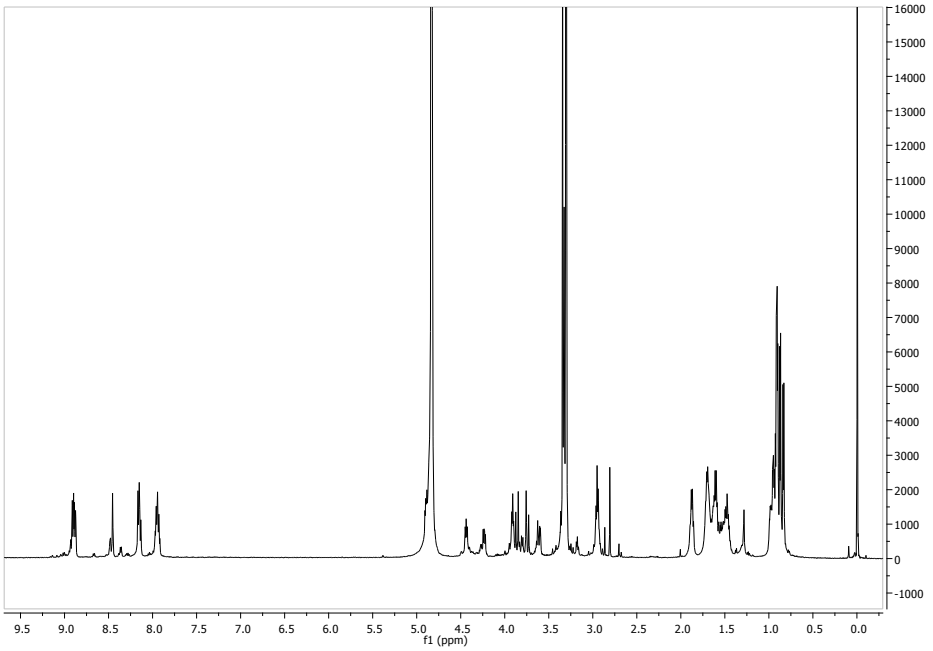
16000
15000
14000
13000
12000
11000
10000
9000
8000
7000
6000
5000
4000
3000
2000
1000
0
-1000
9.5 9.0 8.5 8.0 7.5 7.0 6.5 6.0 5.5 5.0 4.5 4.0 3.5 3.0 2.5 2.0 1.5 1.0 0.5 0.0
f1 (ppm)

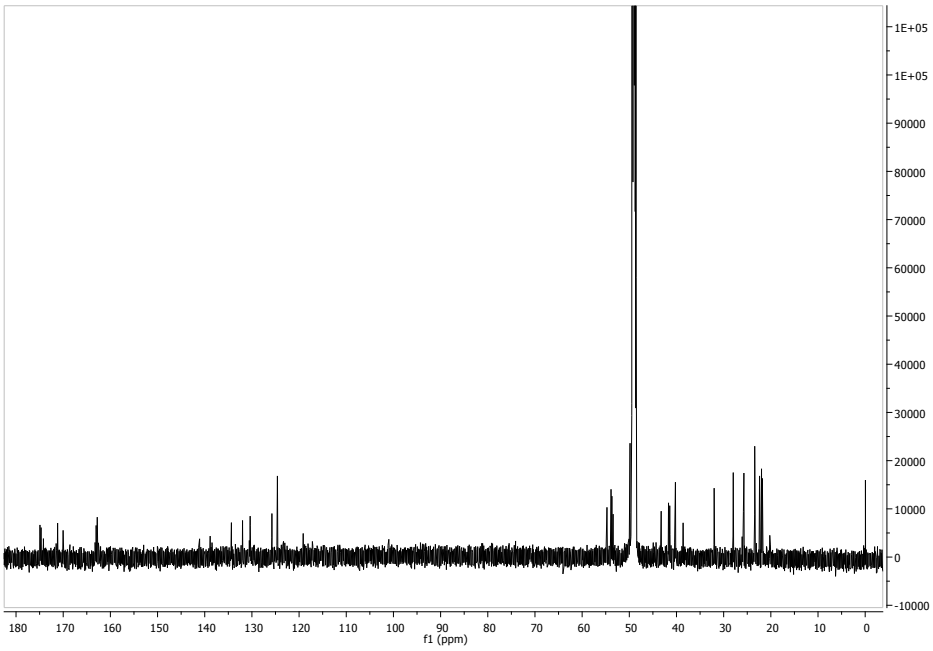
1E+05
1E+05
90000
80000
70000
60000
50000
40000
30000
20000
10000
0
-10000
180 170 160 150 140 130 120 110 100 90 80 70 60 50 40 30 20 10 0
f1 (ppm)

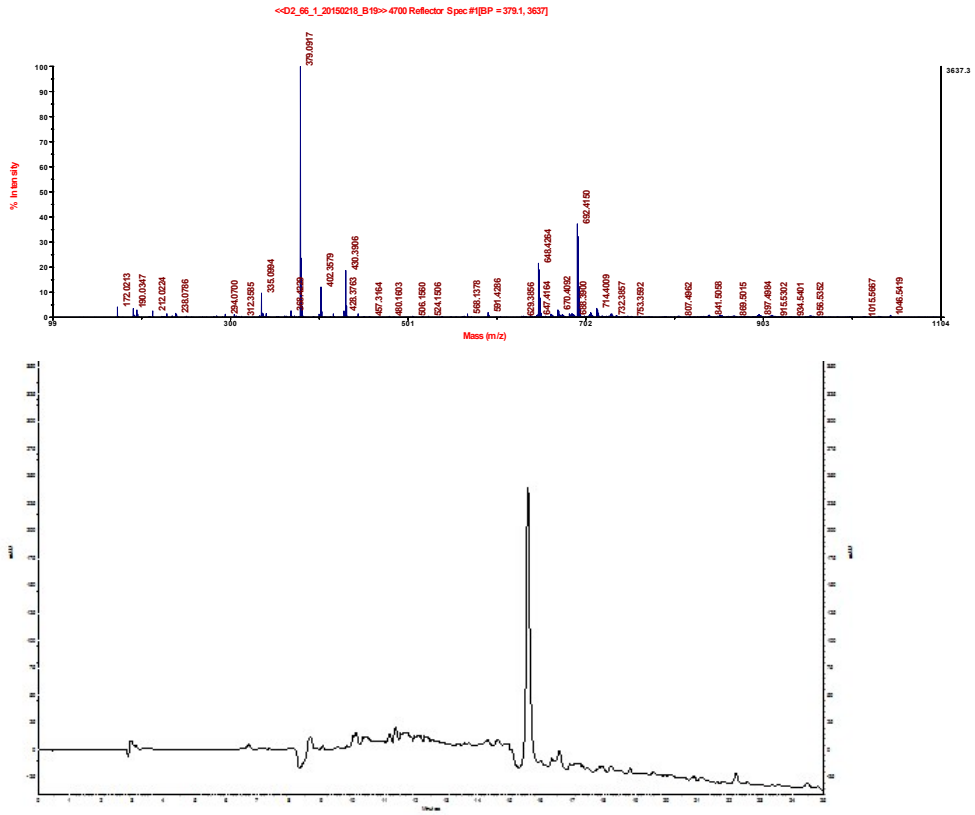

HPLC conditions: Eurospher 100 RP C-18 (150 × 4.5 mm, ID 5 µm) column at flow rate of 0.5 mL/min. λ = 270 nm; mobile phase: 0 min 10 % B, 0-25 min 10 % B-90 % B, 25-30 min 90 % B-50 % B. A = 0.1 % TFA in water, B = 0.1 % TFA in MeOH

Compound **2**

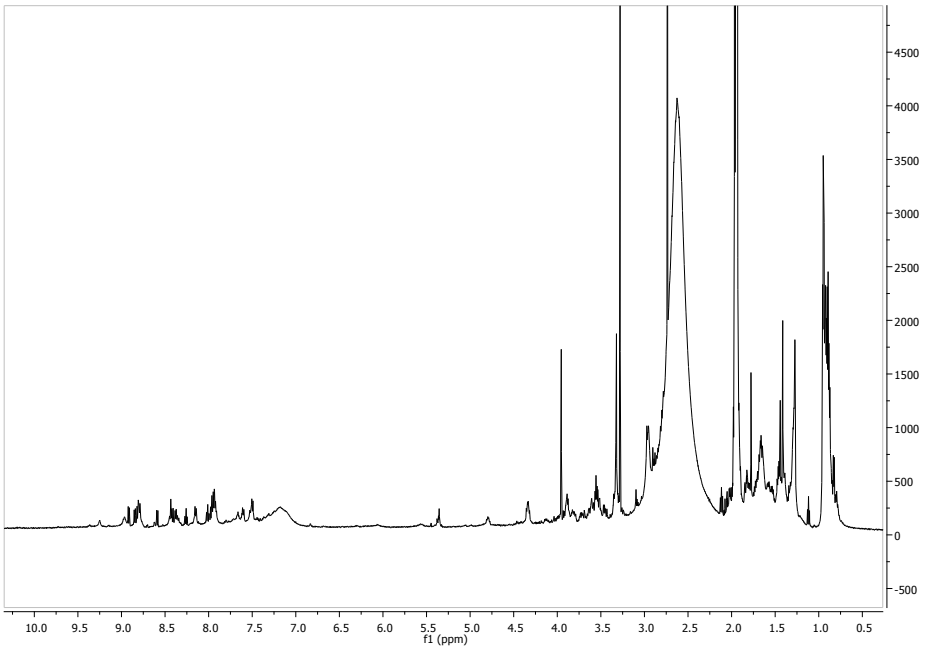

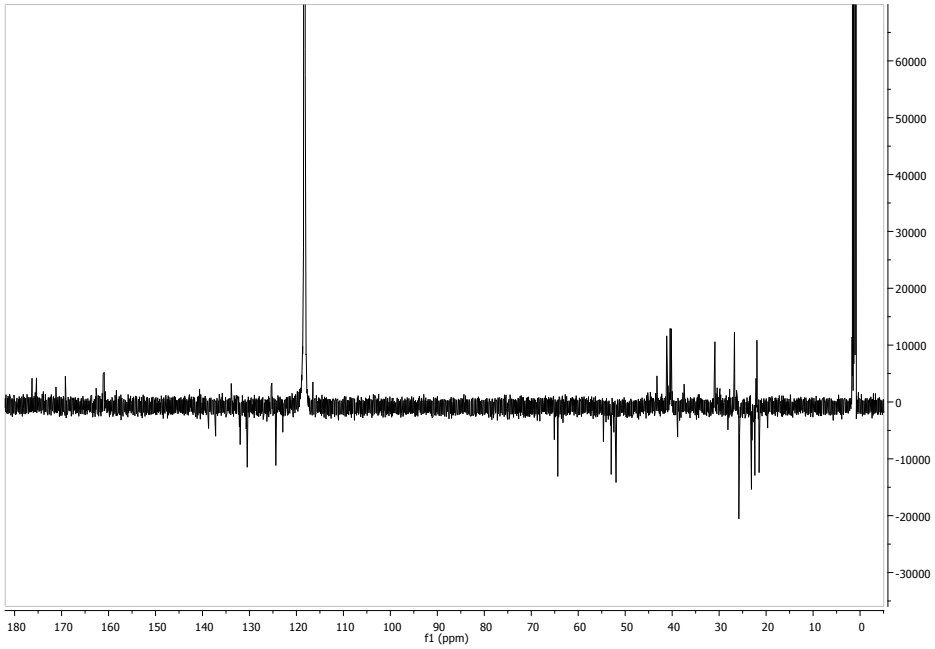

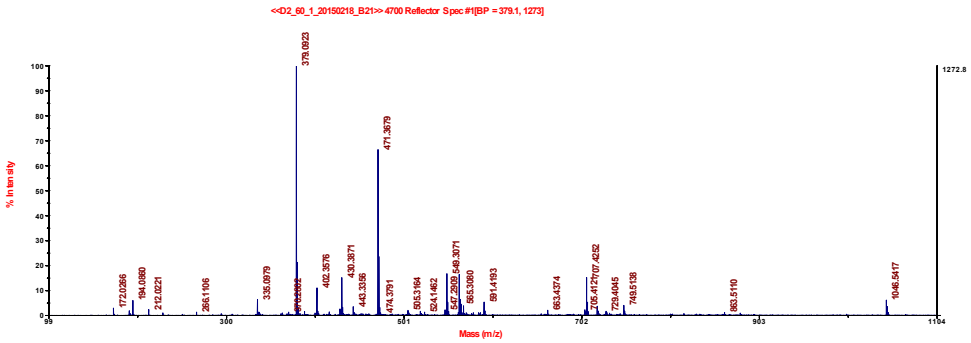

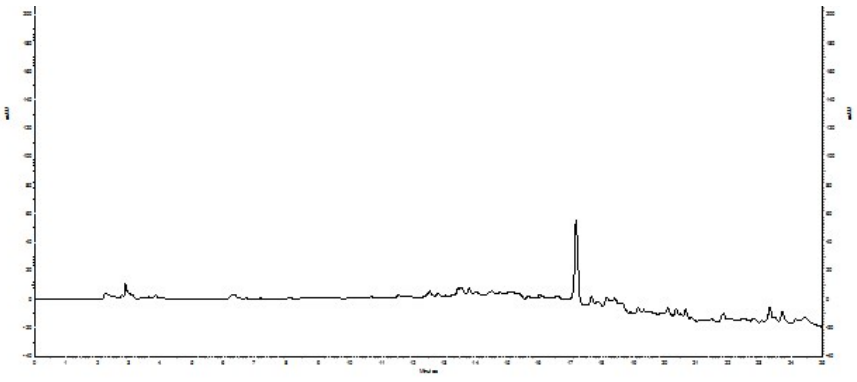

HPLC conditions: Eurospher 100 RP C-18 (150 × 4.5 mm, ID 5 µm) column at flow rate of 0.5 mL/min. λ = 270 nm; mobile phase: 0 min 10 % B, 0-25 min 10 % B-90 % B, 25-30 min 90 % B-50 % B. A = 0.1 % TFA in water, B = 0.1 % TFA in MeOH

Compound **3**

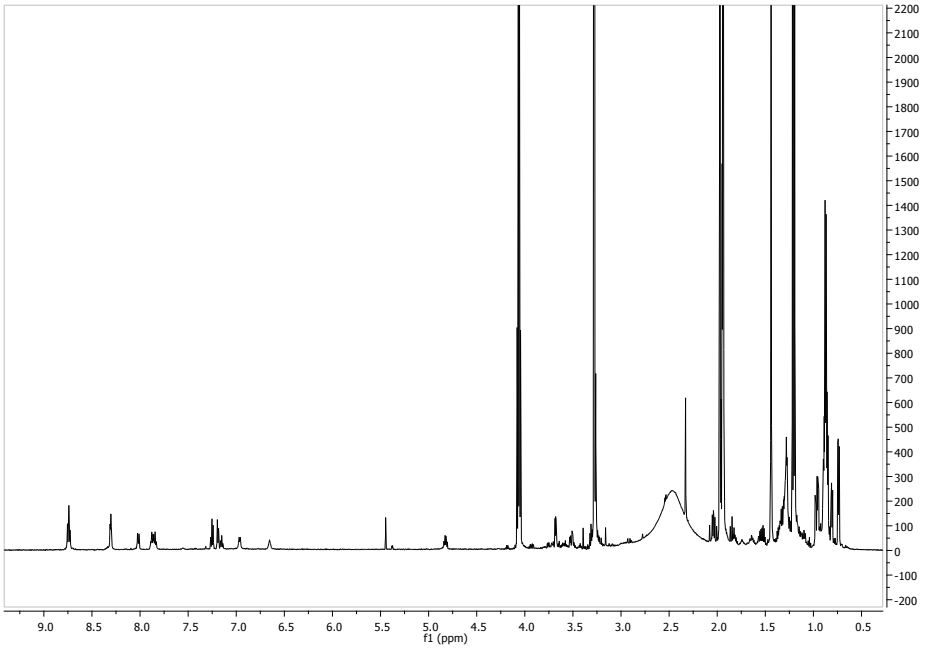

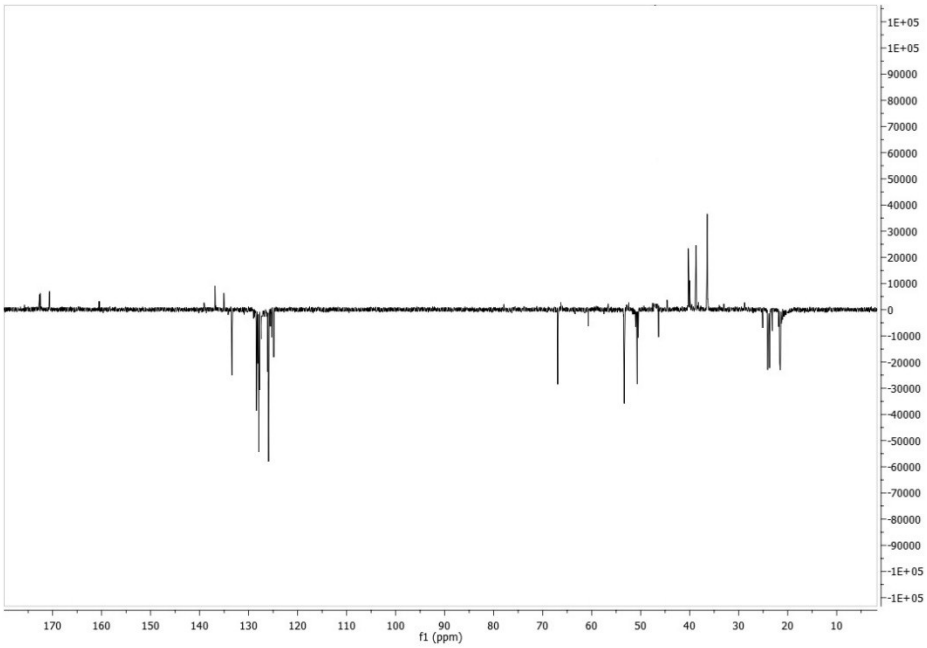

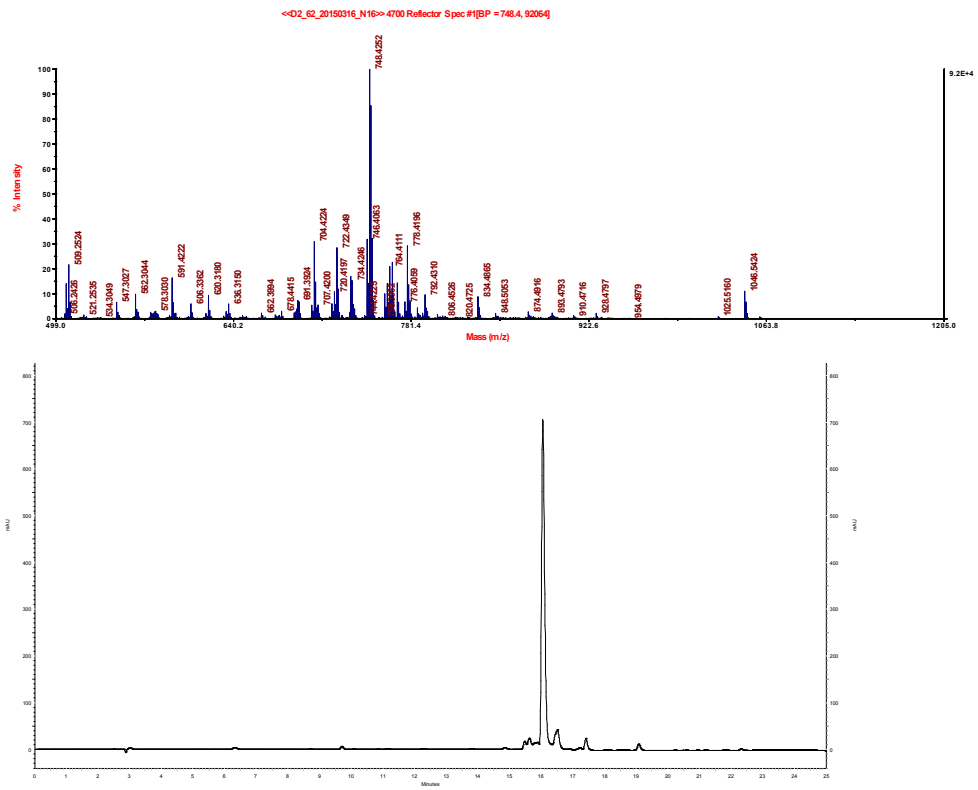

HPLC conditions: Eurospher 100 RP C-18 (150 × 4.5 mm, ID 5 µm) column at flow rate of 0.5 mL/min. λ = 270 nm; mobile phase: 0 min 10 % B, 0-25 min 10 % B-90 % B, 25-30 min 90 % B-50 % B. A = 0.1 % TFA in water, B = 0.1 % TFA in MeOH

Compound **4**

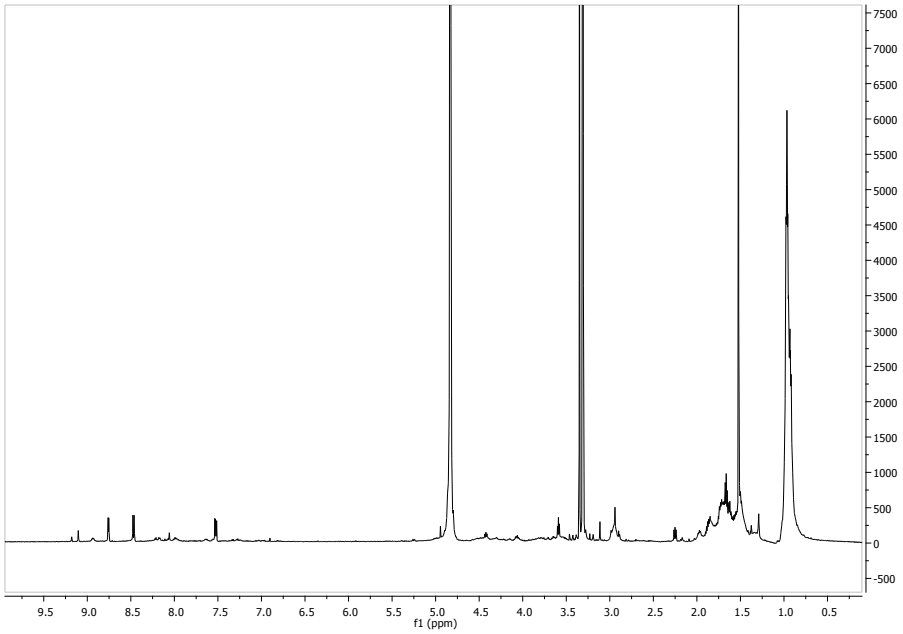

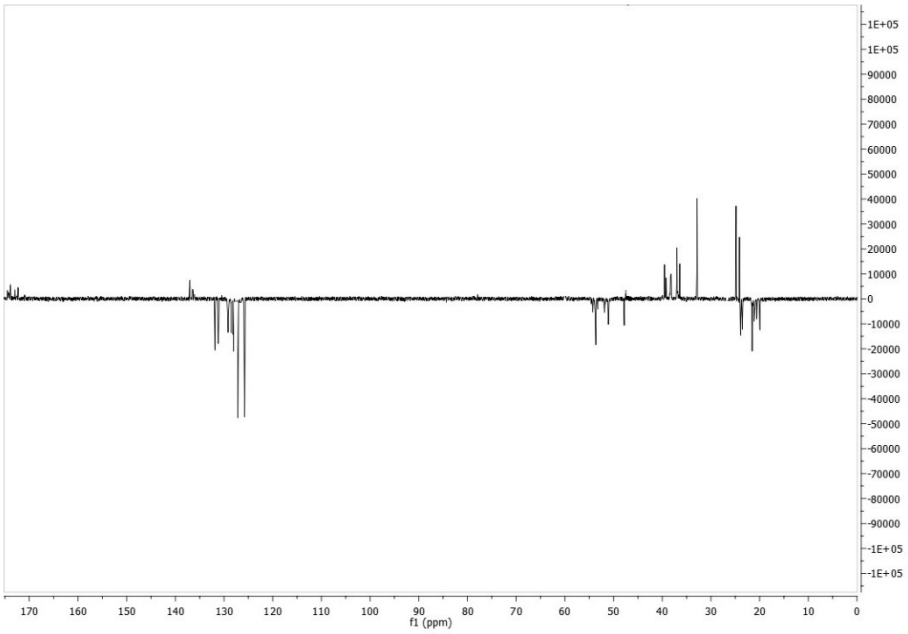

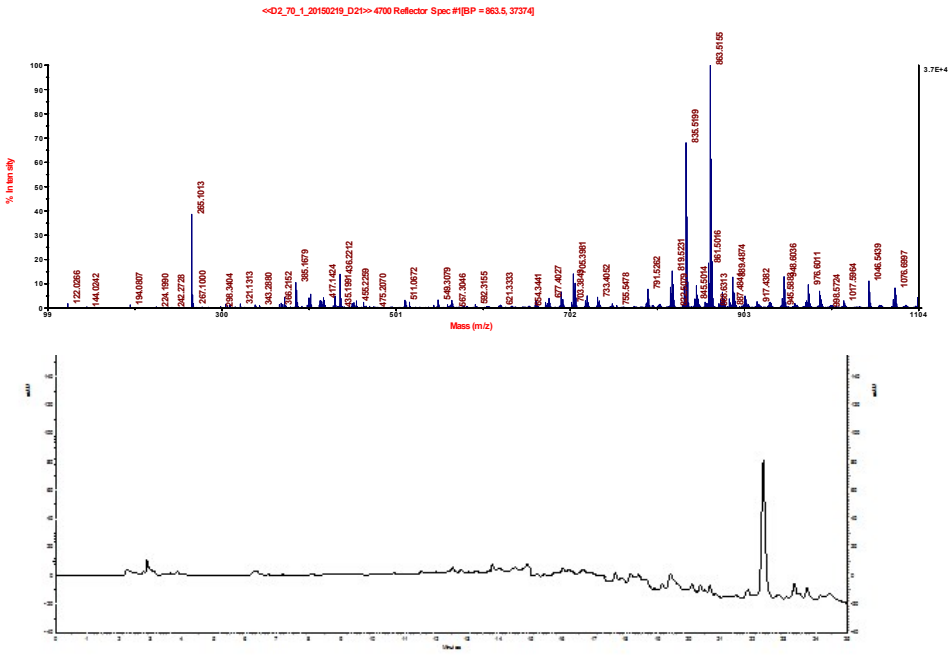

HPLC conditions: Eurospher 100 RP C-18 (150 × 4.5 mm, ID 5 µm) column at flow rate of 0.5 mL/min. λ = 270 nm; mobile phase: 0 min 10 % B, 0-25 min 10 % B-90 % B, 25-30 min 90 % B-50 % B. A = 0.1 % TFA in water, B = 0.1 % TFA in MeOH

2. Spectroscopic properties of 1-4

UV-Vis spectra of compounds **1-4** water solutions found to be almost identical by shape. Due to small amounts of compounds **2-4**, concentrations of their water solutions at pH 7 were determined spectrophotometrically at 251 nm using molar extinction coefficient value (ε=27552 $mmol^{-1}$ cm^2) calculated for **1** at pH 7.

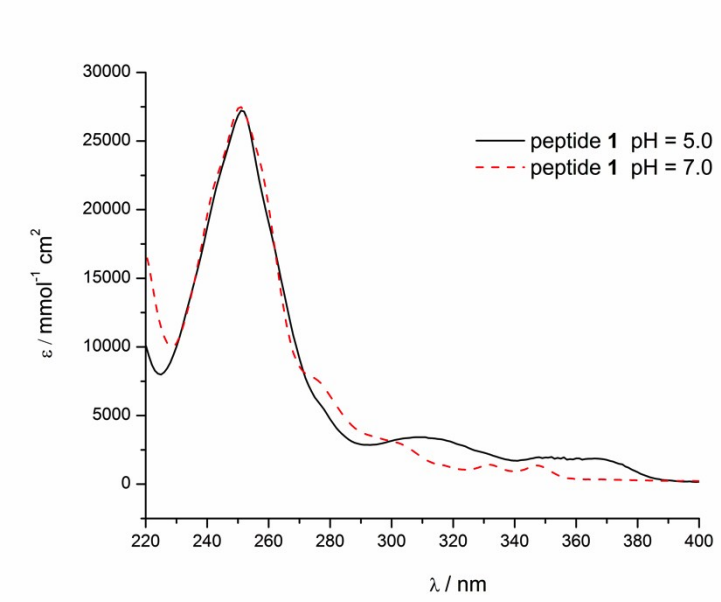

Figure S1. Comparison of UV/Vis spectra of **1** at different conditions: pH 5 (—) and pH 7 (---), c=0.8 – 3 × 10^{-5} M (Na-cacodylate buffer, I=0.05 M)

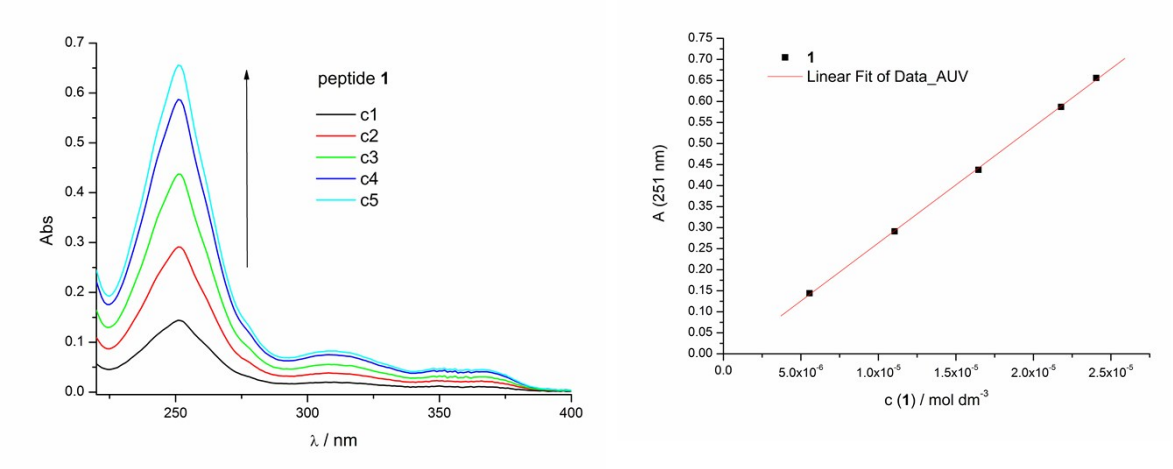

Figure S2. UV/Vis spectra of **1**, *c1-c5*=0.6 – 2.4 × 10^{-5} M (left); linear dependence (—) of the absorbance at 251 nm (■) on the peptide **1** concentration (right), (Na-cacodylate buffer, *I*=0.05 M, pH = 5.0).

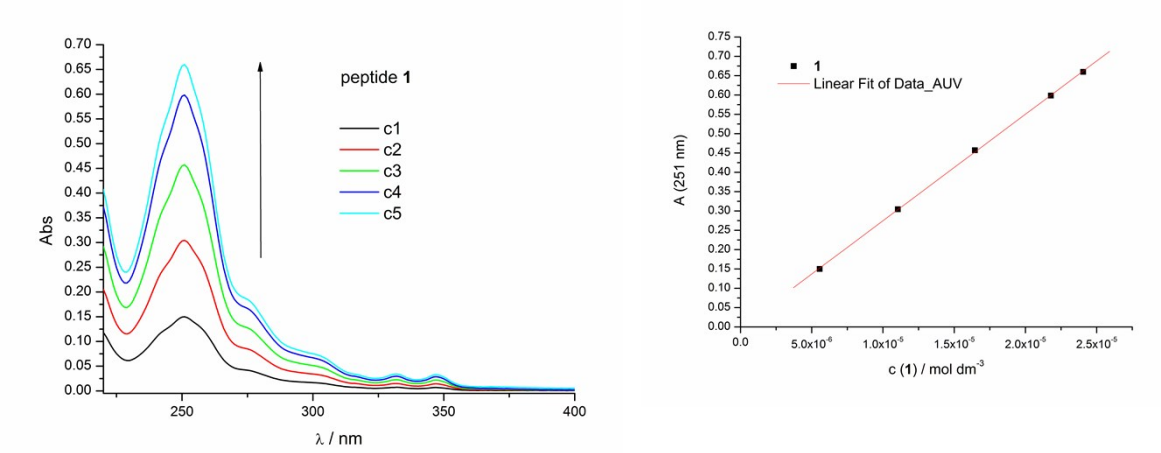

Figure S3. UV/Vis spectra of **1**, *c1-c5*=0.6 – 2.4 × 10^{-5} M (left); linear dependence (—) of the absorbance at 251 nm (■) on the peptide **1** concentration (right), (Na-cacodylate buffer, *I*=0.05 M, pH = 7.0).

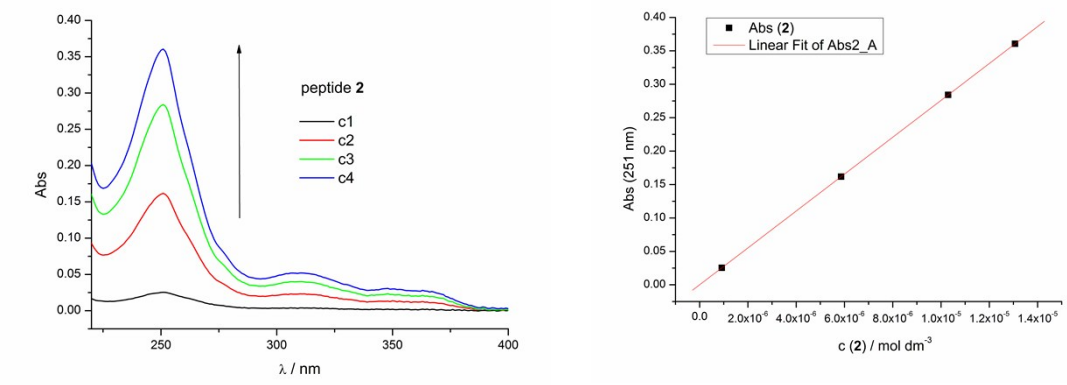

Figure S4. UV/Vis spectra of **2**, *c1-c4*=0.09 – 1.3 × 10^{-5} M (left); linear dependence (—) of the absorbance at 251 nm (■) on the peptide **2** concentration (right), (Na-cacodylate buffer, *I*=0.05 M, pH = 5.0).

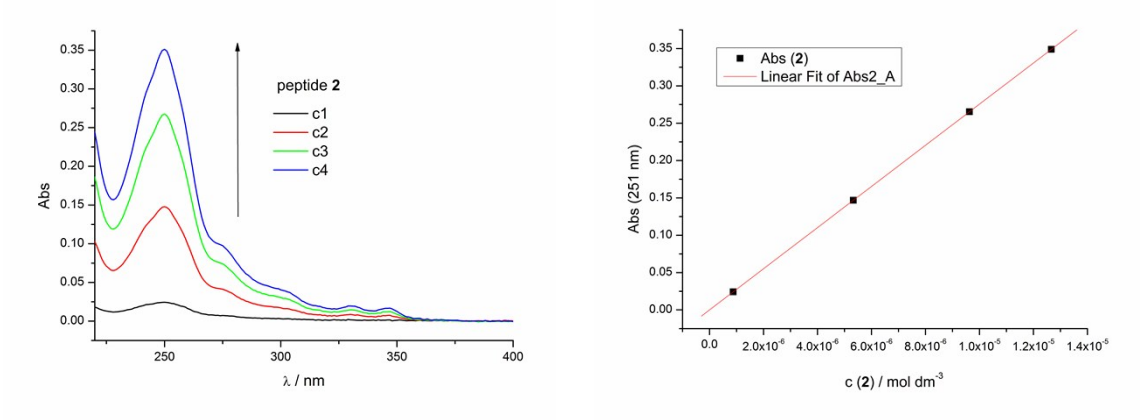

Figure S5. UV/Vis spectra of **2**, *c1-c4*=0.09 – 1.3 × 10^{-5} M (left); linear dependence (—) of the absorbance at 251 nm (■) on the peptide **2** concentration (right), (Na-cacodylate buffer, *I*=0.05 M, pH = 7.0).

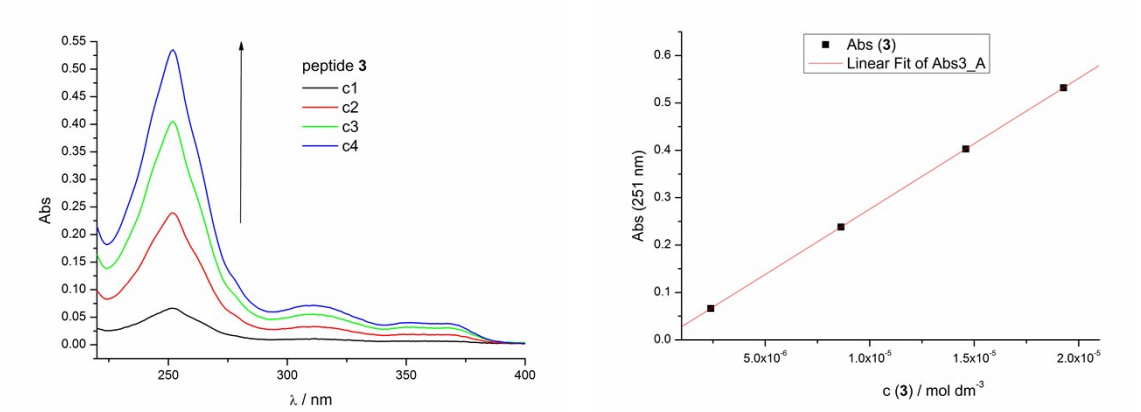

Figure S6. UV/Vis spectra of **3**, *c1-c4*=0.24 – 1.93 × 10^{-5} M (left); linear dependence (—) of the absorbance at 251 nm (■) on the peptide **3** concentration (right), (Na-cacodylate buffer, *I*=0.05 M, pH = 5.0).

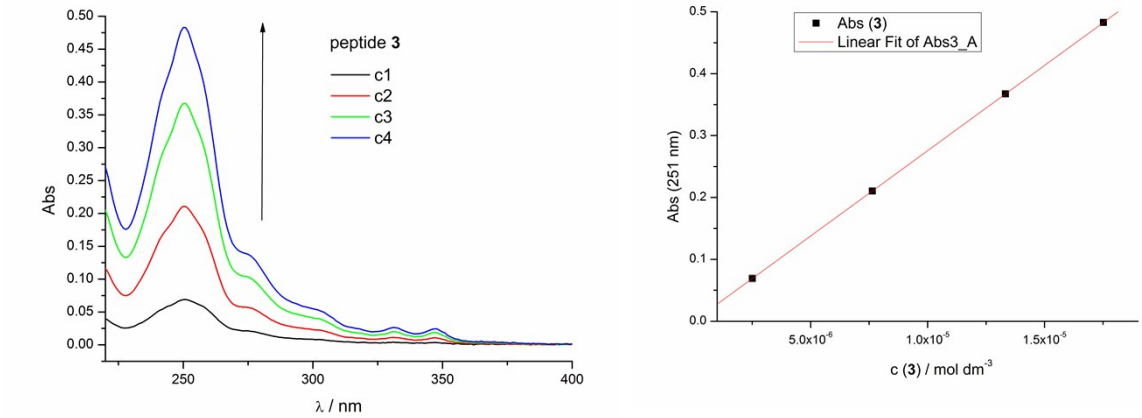

Figure S7. UV/Vis spectra of **3**, *c1-c4*=0.24 – 1.93 × 10^{-5} M (left); linear dependence (—) of the absorbance at 251 nm (■) on the peptide **3** concentration (right), (Na-cacodylate buffer, *I*=0.05 M, pH = 7.0).

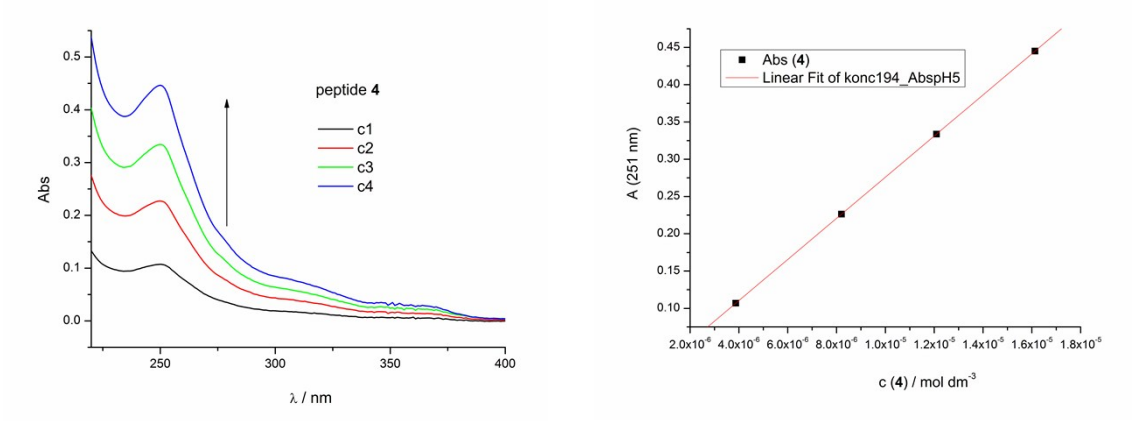

Figure S8. UV/Vis spectra of **4**, *c1-c4*=0.38 – 1.6 × 10^{-5} M (left); linear dependence (—) of the absorbance at 251 nm (■) on the peptide **4** concentration (right), (Na-cacodylate buffer, *I*=0.05 M, pH = 7.0).

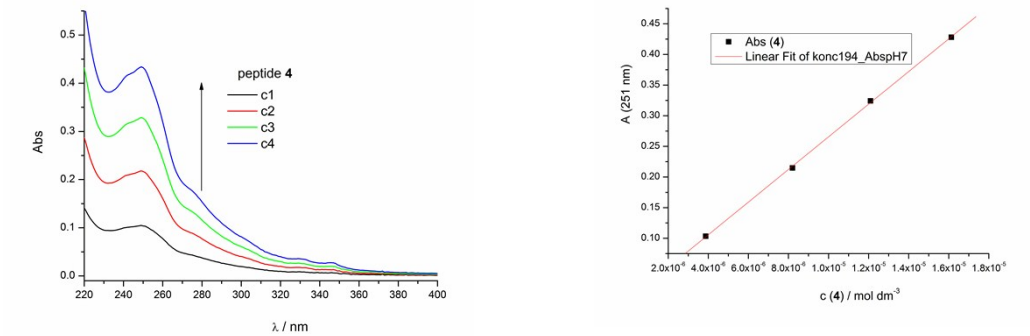

Figure S9. UV/Vis spectra of **4**, *c1-c4*=0.38 – 1.6 × 10^{-5} M (left); linear dependence (—) of the absorbance at 251 nm (■) on the peptide **4** concentration (right), (Na-cacodylate buffer, *I*=0.05 M, pH = 7.0).

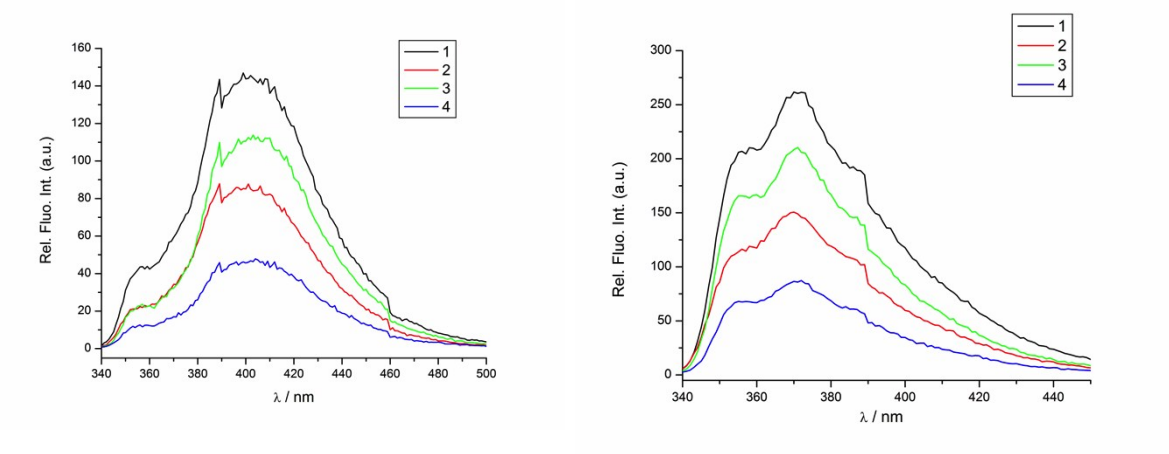

Figure S10. Fluorescence spectra of **1-4** at pH=5.0 (left) and pH=7.0 (right); c=2 ×10^{-6} M, λ_{exc} = 251 nm, (Na-cacodylate buffer, I=0.05 M).

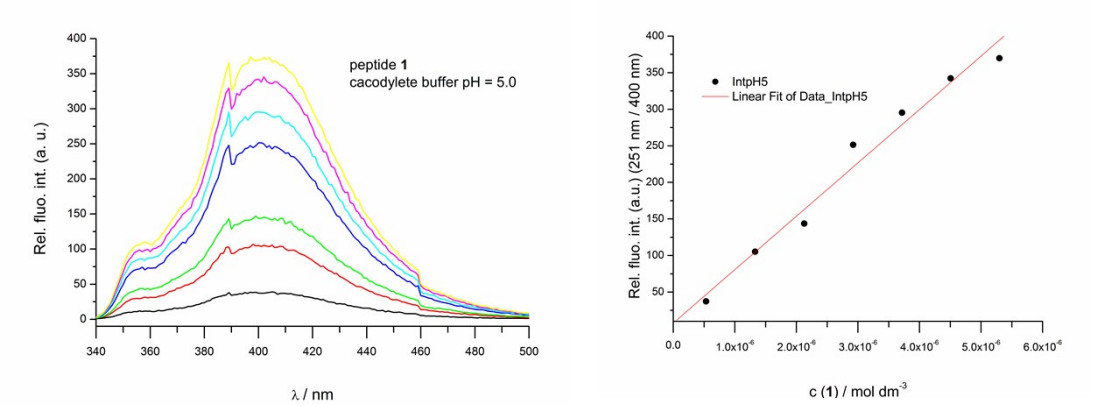

Figure S11. Fluorescence spectra of **1**, λ_{exc} = 251 nm, *c1-c7*=0.5 – 5 × 10^{-6} M (left); linear dependence (—) of the fluorescence intensity λ_{exc} = 251 nm, λ_{em} = 400 nm (■) on the peptide **1** concentration (right), (Na-cacodylate buffer, I=0.05 M, pH = 5.0).

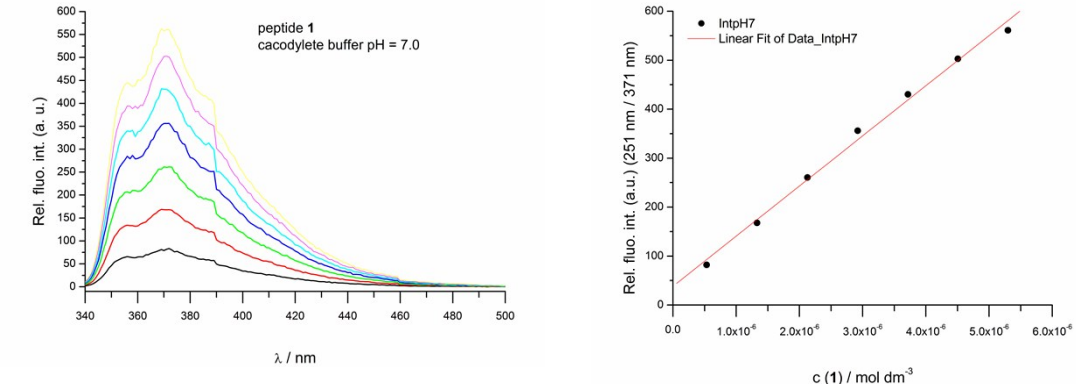

Figure S12. Fluorescence spectra of **1**, λ_{exc} = 251 nm, *c1*-*c7*=0.5 – 5 × 10^{-6} M (left); linear dependence (—) of the fluorescence intensity λ_{exc} = 251 nm, λ_{em} = 371 nm (■) on the peptide **1** concentration (right), (Na-cacodylate buffer, *I*=0.05 M, pH = 7.0).

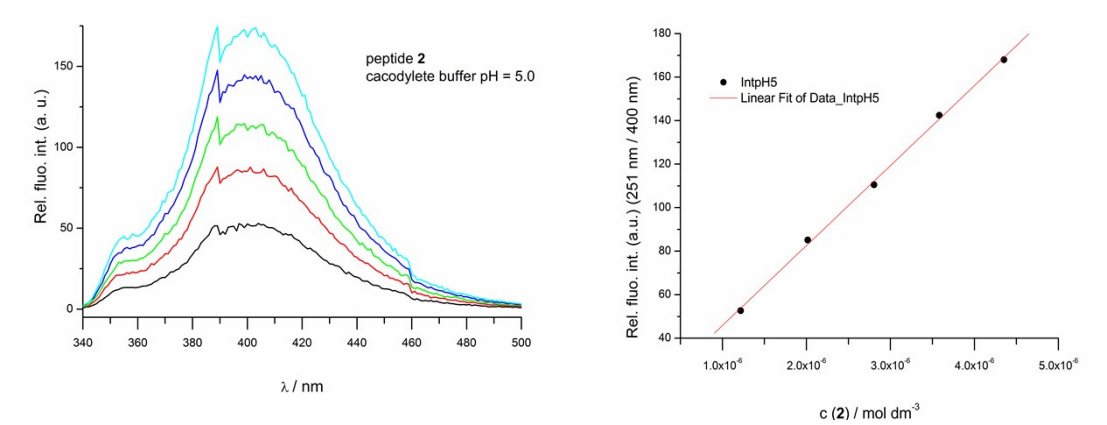

Figure S13. Fluorescence spectra of **2**, λ_{exc} = 251 nm, *c1*-*c5*=1.2 – 4.3 × 10^{-6} M (left); linear dependence (—) of the fluorescence intensity λ_{exc} = 251 nm, λ_{em} = 400 nm (■) on the peptide **2** concentration (right), (Na-cacodylate buffer, *I*=0.05 M, pH = 5.0).

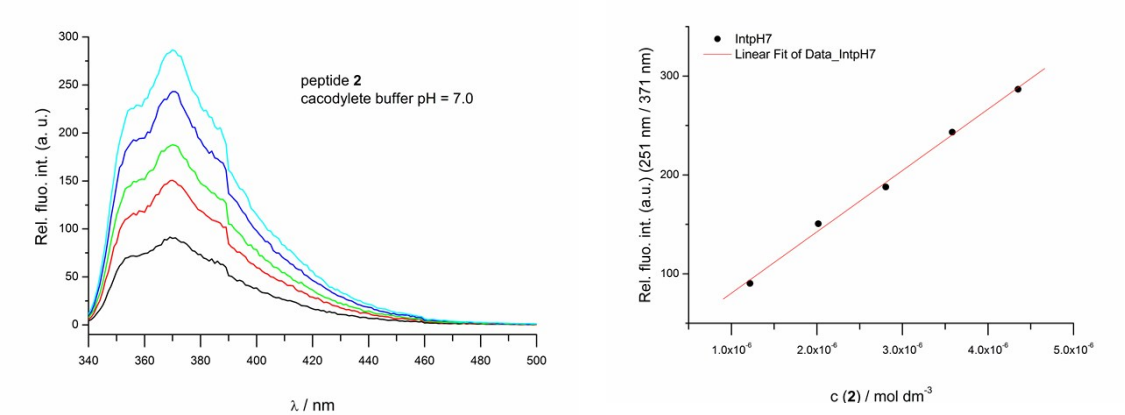

Figure S14. Fluorescence spectra of **2**, λ_{exc} = 251 nm, *c1*-*c5*=1.2 – 4.3 × 10^{-6} M (left); linear dependence (—) of the fluorescence intensity λ_{exc} = 251 nm, λ_{em} = 371 nm (■) on the peptide **2** concentration (right), (Na-cacodylate buffer, *I*=0.05 M, pH = 7.0).

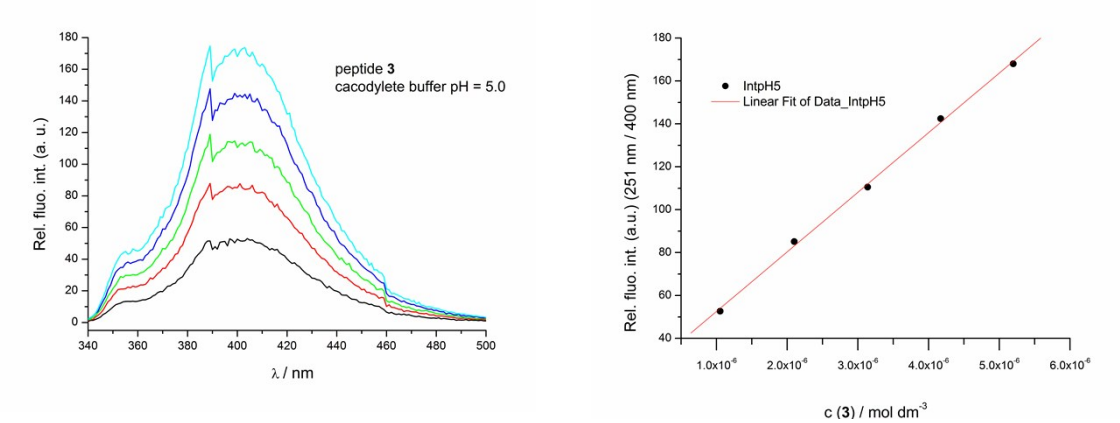

Figure S15. Fluorescence spectra of **3**, λ_{exc} = 251 nm, *c1-c5*=1.0 – 5.2 × 10^{-6} M (left); linear dependence (—) of the fluorescence intensity λ_{exc} = 251 nm, λ_{em} = 400 nm (■) on the peptide **3** concentration (right), (Na-cacodylate buffer, *I*=0.05 M, pH = 5.0).

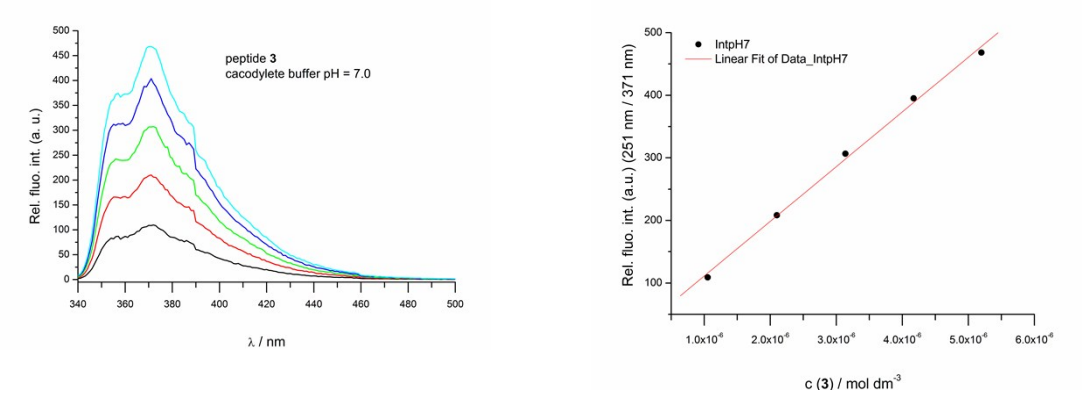

Figure S16. Fluorescence spectra of **3**, λ_{exc} = 251 nm, *c1-c5*=1.0 – 5.2 × 10^{-6} M (left); linear dependence (—) of the fluorescence intensity λ_{exc} = 251 nm, λ_{em} = 371 nm (■) on the peptide **3** concentration (right), (Na-cacodylate buffer, *I*=0.05 M, pH = 7.0).

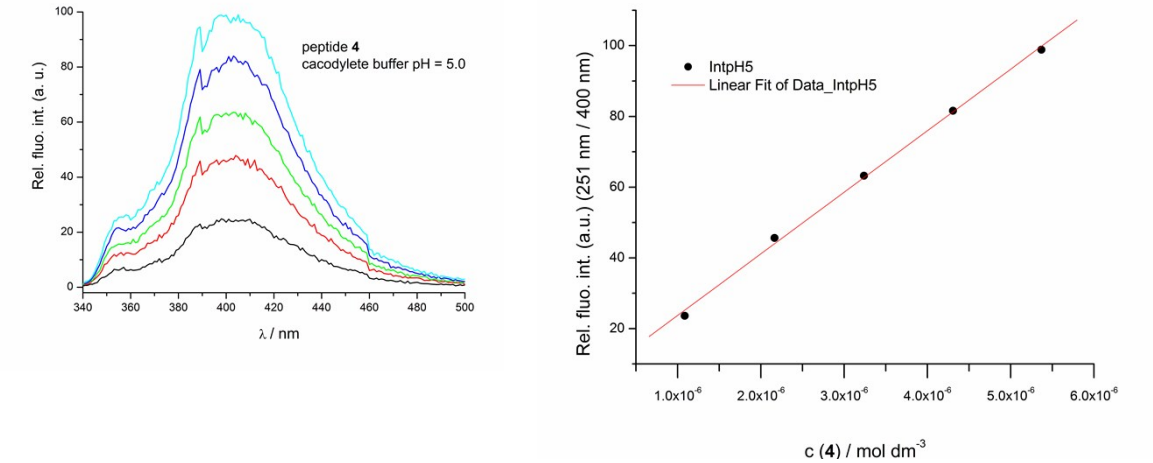

Figure S17. Fluorescence spectra of **4**, λ_{exc} = 251 nm, *c1-c5*=1.1 – 5.4 × 10^{-6} M (left); linear dependence (—) of the fluorescence intensity λ_{exc} = 251 nm, λ_{em} = 400 nm (■) on the peptide **4** concentration (right), (Na-cacodylate buffer, *I*=0.05 M, pH = 5.0).

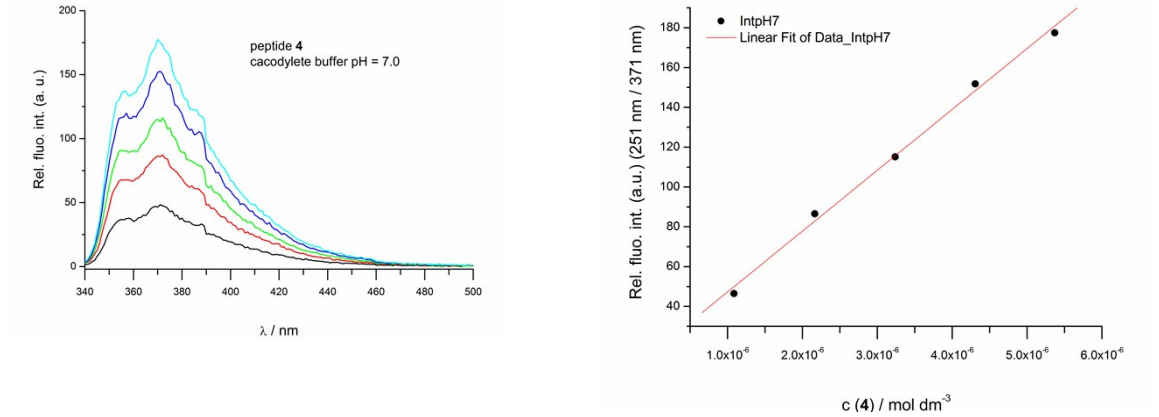

Figure S18. Fluorescence spectra of **4**, λ_{exc} = 251 nm, *c1-c5*=1.1 – 5.4 × 10^{-6} M (left); linear dependence (—) of the fluorescence intensity λ_{exc} = 251 nm, λ_{em} = 371 nm (■) on the peptide **4** concentration (right), (Na-cacodylate buffer, *I*=0.05 M, pH = 7.0).

3. Interactions of 1-4 with DNA/RNA

3.1. Thermal melting experiments

Table S1. The [a]ΔT_m values (°C) of studied ds-polynucleotides upon addition of **1-4** (ratio r^{b} = 0.3) at pH = 5.0 and pH = 7.0 (buffer sodium cacodylate, I = 0.05 mol dm^{-3}), c(DNA / RNA) = 1-2 ×10^{-5} M.

	ΔTm / °C					
Compound	***ct*-DNA**		**poly dAdT – poly dAdT**		**poly rA – poly rU**	
	pH 5	pH 7	pH 5	pH 7	pH 5	pH 7
1	1.5	0	2.8	0	-2.4/-0.7 [c]	0.7
2	0	-0.8	0.8	-0.5	-1.0/-0.8 [c]	0
3	0	0	-0.6	-0.7	0/-0.8 [c]	0
4	0	0	-0.7	-0.8	0/-0.5 [c]	0

[a] Error in ΔT_m : ± 0.5°C;
[b] r = [compound] / [polynucleotide];
[c] biphasic transitions: the first transition at T_m = 48 °C is attributed to denaturation of poly rA-poly rU and the second transition at T_m = 71 °C is attributed to denaturation of poly rAH$^+$-poly rAH$^+$ since poly rA at pH=5 is mostly protonated and forms ds-polynucleotide. [1]

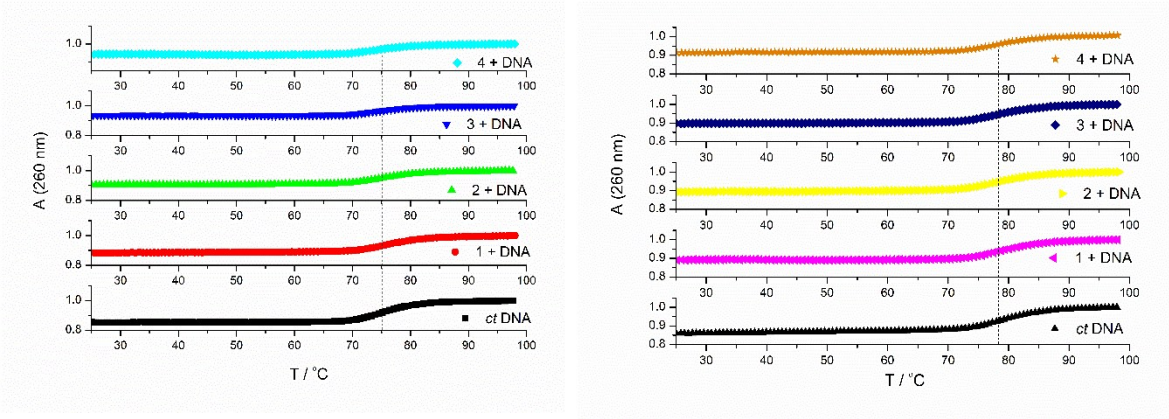

Figure S19. Melting curves of *ct*-DNA upon addition of **1-4** (c (*ct*-DNA)= 1-2 ×10^{-5} M; ratio $r_{[compound] / [polynucleotide]}$ = 0.3) at pH = 5.0 (left) and pH = 7.0 (right) (sodium cacodylate buffer, I = 0.05 mol dm^{-3})

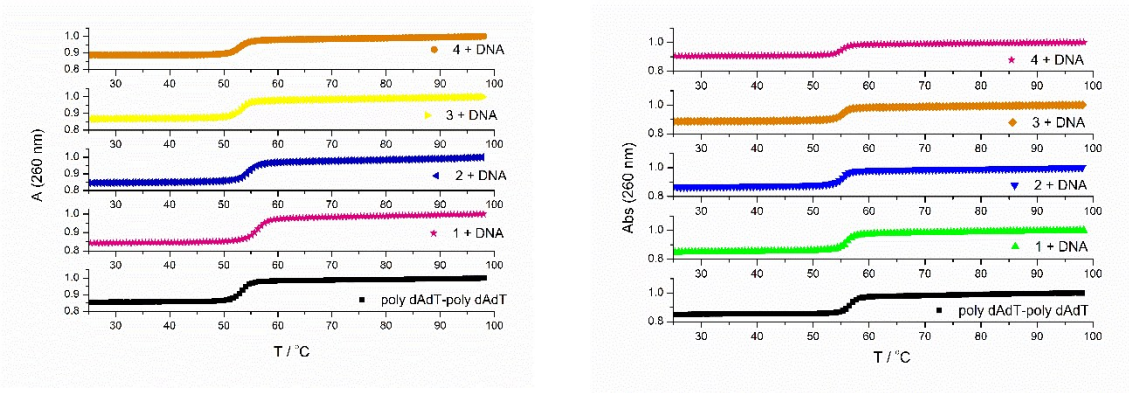

Figure S20. Melting curves of poly dAdT-poly dAdT upon addition of **1-4** (c (poly dAdT-poly dAdT)= 1.5 $\times 10^{-5}$ M; ratio $r_{[\text{compound}]\ /\ [\text{polynucleotide}]}$ = 0.3) at pH = 5.0 (left) and pH = 7.0 (right) (sodium cacodylate buffer, I = 0.05 mol dm^{-3})

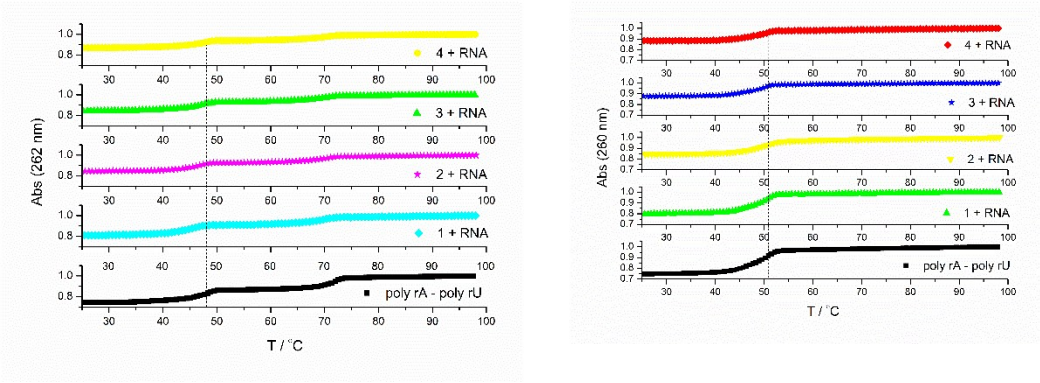

Figure S21. Melting curves of poly rA-poly rU upon addition of **1-4** (c (poly rA-poly rU)= 1.5-2.2 $\times 10^{-5}$ M; ratio $r_{[\text{compound}]\ /\ [\text{polynucleotide}]}$ = 0.3) at pH = 5.0 (left) and pH = 7.0 (right) (sodium cacodylate buffer, I = 0.05 mol dm^{-3})

3.2. Circular dichroism (CD) experiments

In order to get insight into the changes of polynucleotide properties induced by small molecule binding, we have chosen CD spectroscopy as a highly sensitive method toward conformational changes in the secondary structure of polynucleotides.[2] Compounds **1-4** possess chiral atoms and consequently have intrinsic CD spectrum.

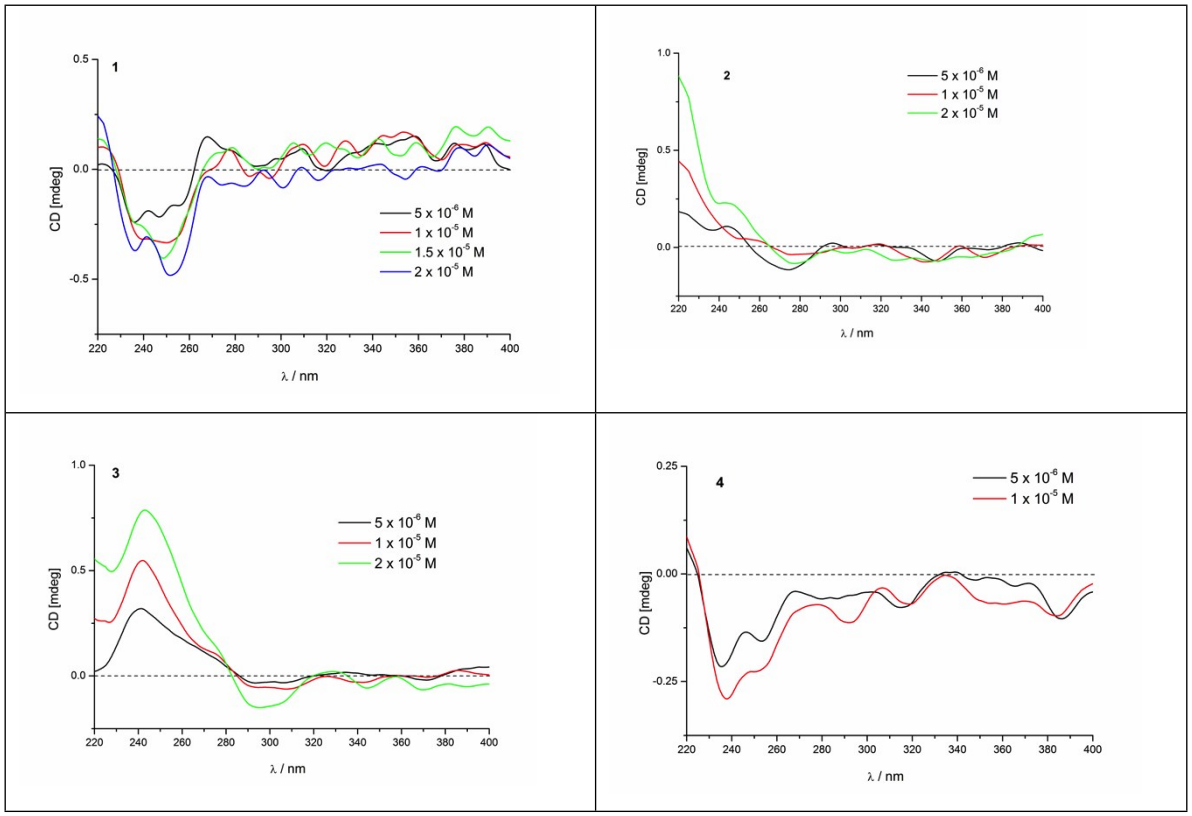

Figure S22. CD spectra of **1-4**, Na-cacodylate buffer, **pH 5.0**, *I*= 0.05 M

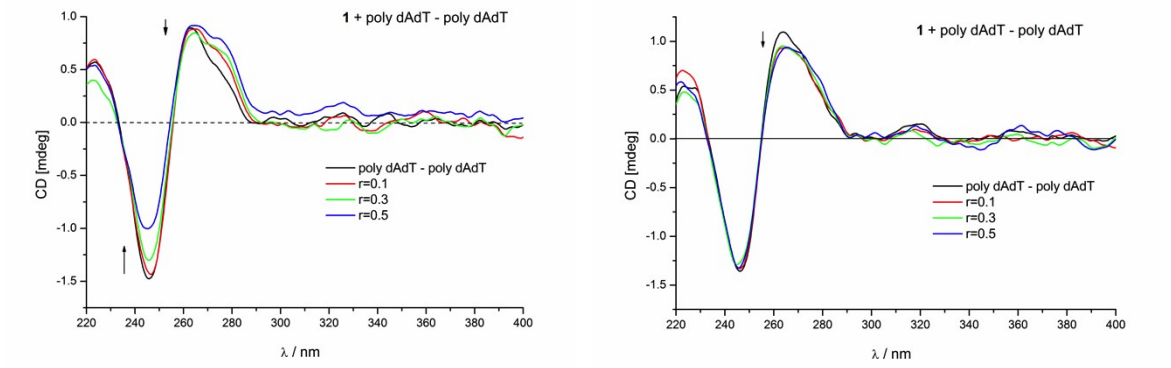

Figure S23. Changes in the CD spectrum of poly dAdT-poly dAdT (c = 2.0 × 10^{-5} moldm^{-3}) upon addition of **1** at different molar ratios ***r*** = [compound] / [polynucleotide], **pH = 5.0** (left) and **pH=7.0** (right), sodium cacodylate buffer, I = 0.05 moldm^{-3}.

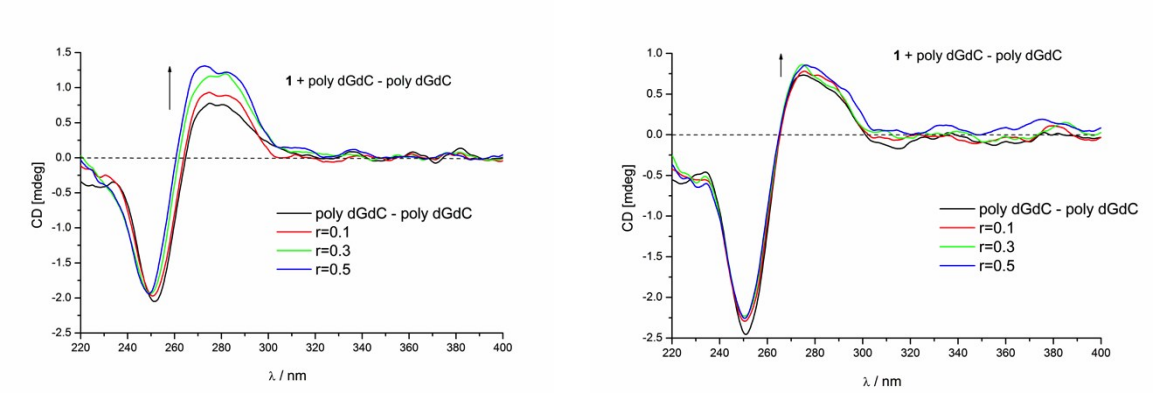

Figure S24. Changes in the CD spectrum of poly dGdC-poly dGdC (c = 2.0 × 10^{-5} mol dm^{-3}) upon addition of **1** at different molar ratios ***r*** = [compound] / [polynucleotide], **pH = 5.0** (left) and **pH=7.0** (right), sodium cacodylate buffer, I = 0.05 mol dm^{-3}.

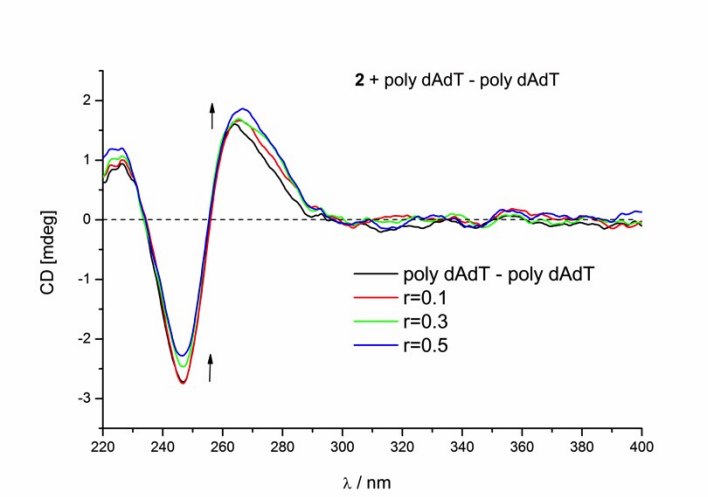

Figure S25. Changes in the CD spectrum of poly dAdT-poly dAdT (c = 2.0 × 10^{-5} mol dm^{-3}) upon addition of **2** at different molar ratios ***r*** = [compound] / [polynucleotide], **pH = 5.0**, sodium cacodylate buffer, I = 0.05 mol dm^{-3}.

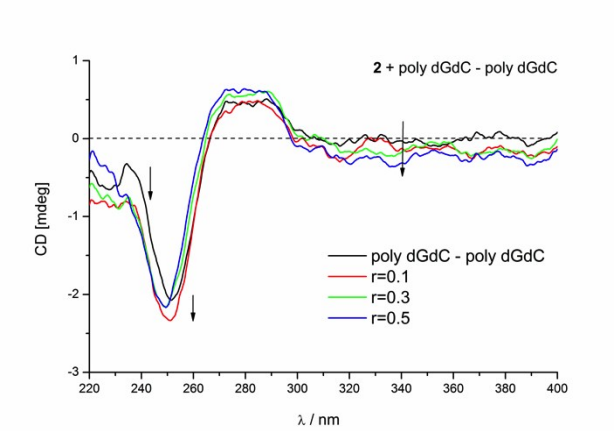

Figure S26. Changes in the CD spectrum of poly dGdC-poly dGdC (c = 2.0 × 10^{-5} mol dm^{-3}) upon addition of **2** at different molar ratios ***r*** = [compound] / [polynucleotide], **pH = 5.0**, sodium cacodylate buffer, I = 0.05 mol dm^{-3}.

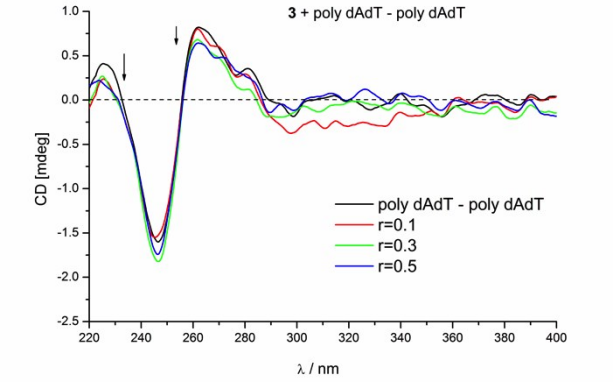

Figure S27. Changes in the CD spectrum of poly dAdT-poly dAdT (c = 2.0 × 10^{-5} mol dm^{-3}) upon addition of **3** at different molar ratios ***r*** = [compound] / [polynucleotide], **pH = 5.0**, sodium cacodylate buffer, I = 0.05 mol dm^{-3}.

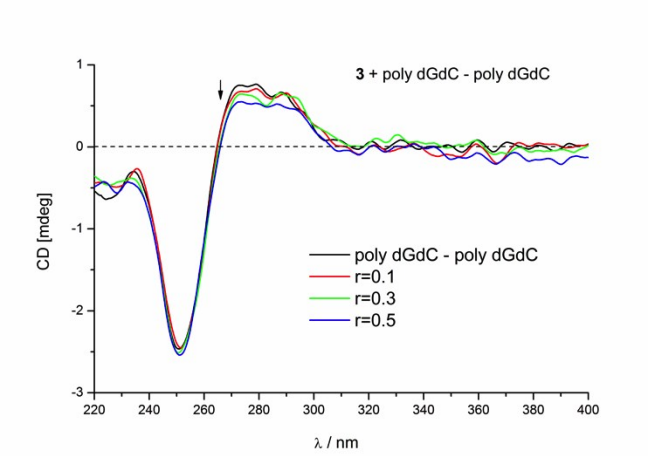

Figure S28. Changes in the CD spectrum of poly dGdC-poly dGdC (c = 2.0 × 10^{-5} mol dm^{-3}) upon addition of **3** at different molar ratios ***r*** = [compound] / [polynucleotide], **pH = 5.0**, sodium cacodylate buffer, I = 0.05 mol dm^{-3}.

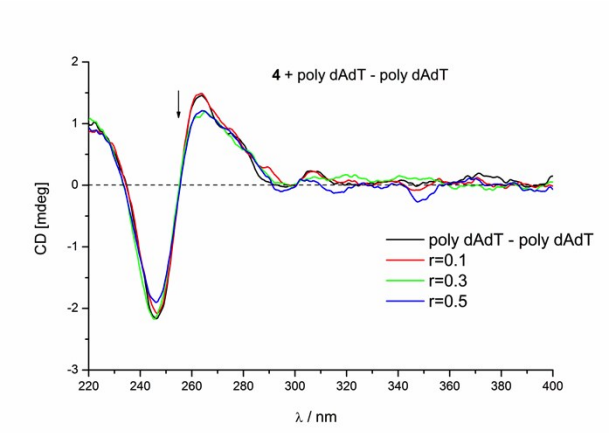

Figure S29. Changes in the CD spectrum of poly dAdT-poly dAdT (c = 2.0 × 10^{-5} mol dm^{-3}) upon addition of **4** at different molar ratios ***r*** = [compound] / [polynucleotide], **pH = 5.0**, sodium cacodylate buffer, I = 0.05 mol dm^{-3}.

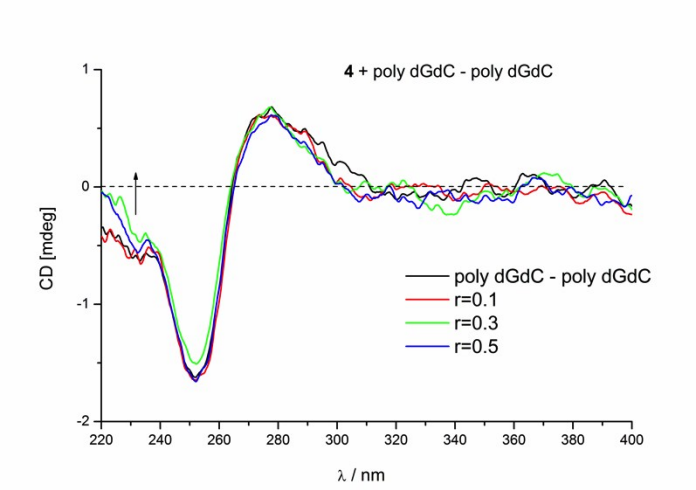

Figure S30. Changes in the CD spectrum of poly dGdC-poly dGdC (c = 2.0 × 10^{-5} mol dm^{-3}) upon addition of **4** at different molar ratios ***r*** = [compound] / [polynucleotide], **pH = 5.0**, sodium cacodylate buffer, I = 0.05 mol dm^{-3}.

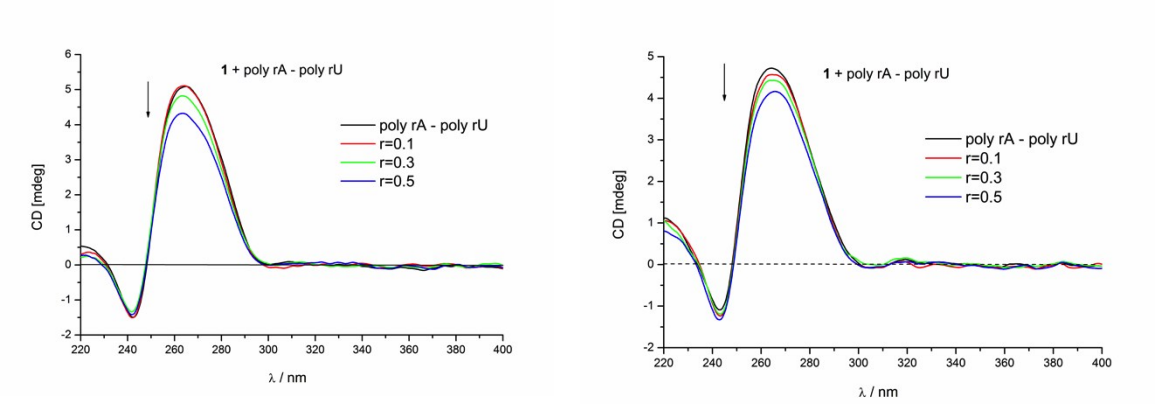

Figure S31. Changes in the CD spectrum of poly rA-poly rU (c = 2.0 × 10^{-5} mol dm^{-3}) upon addition of **1** at different molar ratios ***r*** = [compound] / [polynucleotide], **pH = 5.0** (left) and **pH=7.0** (right), sodium cacodylate buffer, I = 0.05 mol dm^{-3}.

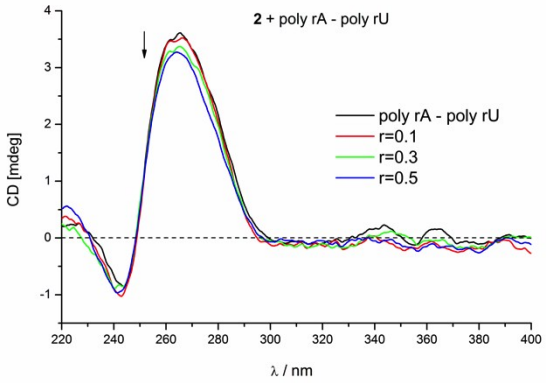

Figure S32. Changes in the CD spectrum of poly rA-poly rU (c = 2.0 × 10^{-5} mol dm^{-3}) upon addition of **2** at different molar ratios ***r*** = [compound] / [polynucleotide], **pH = 5.0**, sodium cacodylate buffer, I = 0.05 mol dm^{-3}.

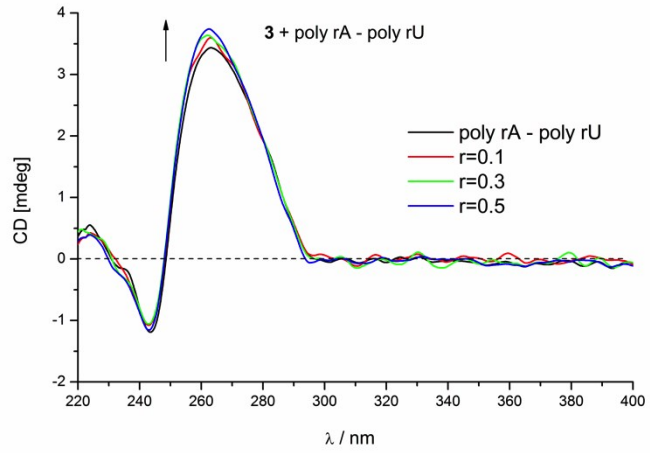

Figure S33. Changes in the CD spectrum of poly rA-poly rU (c = 2.0 × 10^{-5} mol dm^{-3}) upon addition of **3** at different molar ratios ***r*** = [compound] / [polynucleotide], **pH = 5.0**, sodium cacodylate buffer, I = 0.05 mol dm^{-3}.

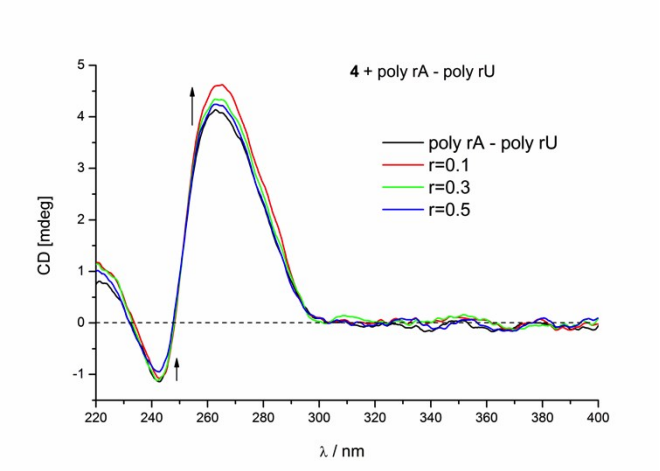

Figure S34. Changes in the CD spectrum of poly rA-poly rU (c = 2.0 × 10^{-5} mol dm^{-3}) upon addition of **4** at different molar ratios ***r*** = [compound] / [polynucleotide], **pH = 5.0**, sodium cacodylate buffer, I = 0.05 mol dm^{-3}.

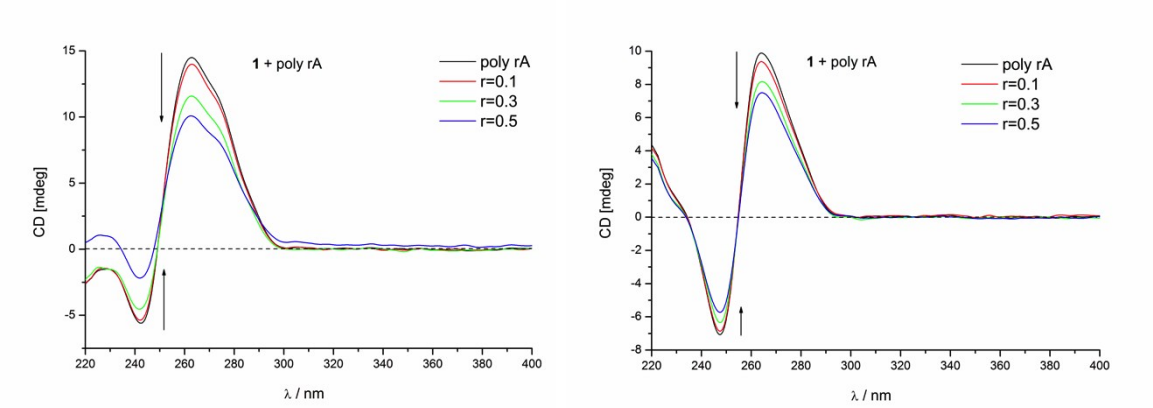

Figure S35. Changes in the CD spectrum of poly rA (c = 2.0 × 10^{-5} mol dm^{-3}) upon addition of **1** at different molar ratios ***r*** = [compound] / [polynucleotide], **pH = 5.0** (left) and **pH=7.0** (right), sodium cacodylate buffer, I = 0.05 mol dm^{-3}.

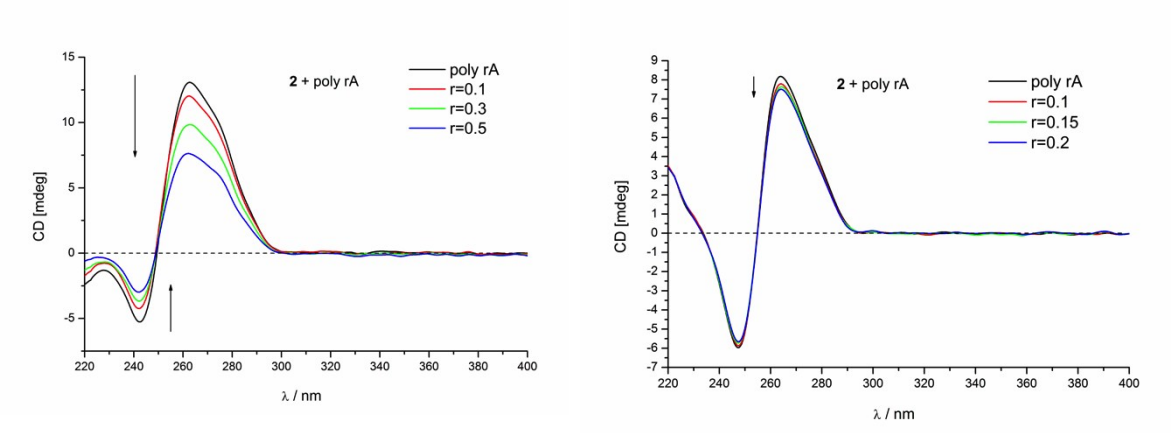

Figure S36. Changes in the CD spectrum of poly rA (c = 2.0 × 10^{-5} mol dm^{-3}) upon addition of **2** at different molar ratios ***r*** = [compound] / [polynucleotide], **pH = 5.0** (left) and **pH=7.0** (right), sodium cacodylate buffer, I = 0.05 mol dm^{-3}.

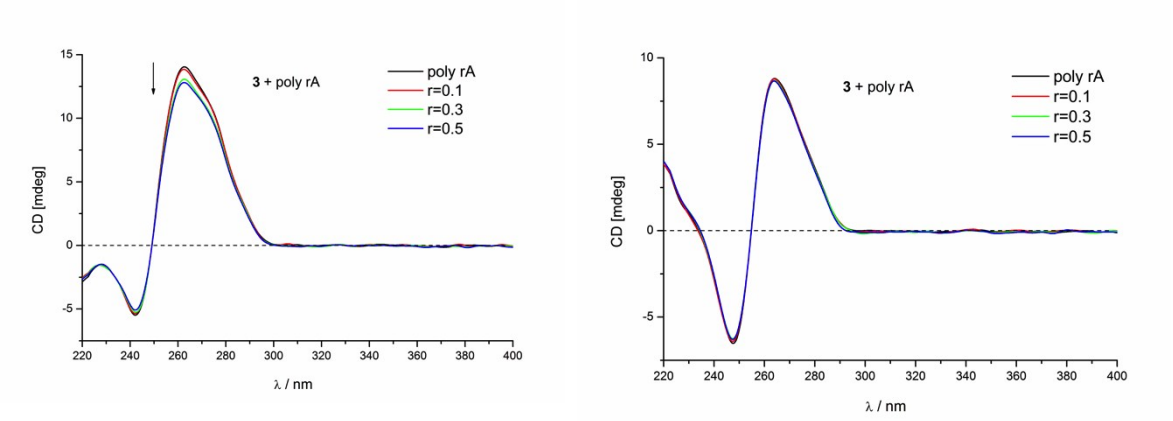

Figure S37. Changes in the CD spectrum of poly rA (c = 2.0 × 10^{-5} mol dm^{-3}) upon addition of **3** at different molar ratios ***r*** = [compound] / [polynucleotide], **pH = 5.0** (left) and **pH=7.0** (right), sodium cacodylate buffer, I = 0.05 mol dm^{-3}.

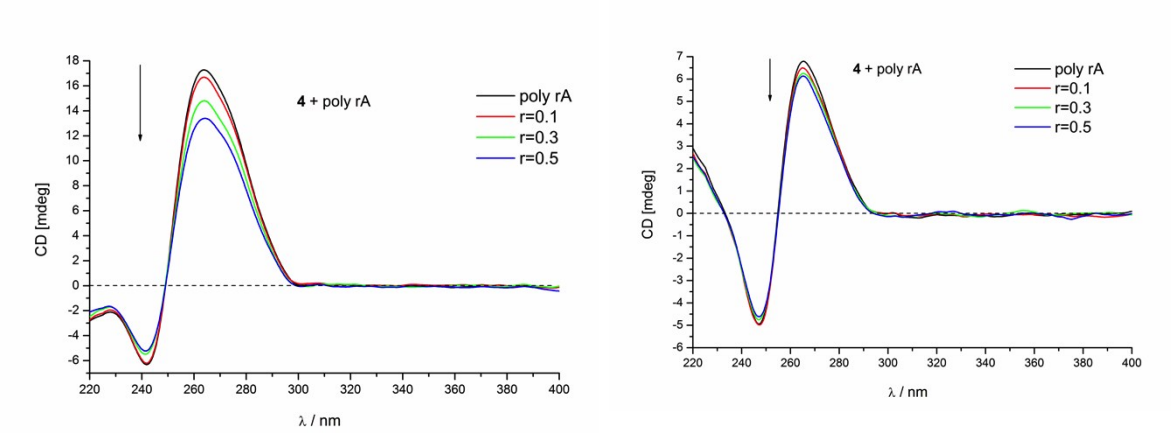

Figure S38. Changes in the CD spectrum of poly rA (c = 2.0 × 10^{-5} mol dm^{-3}) upon addition of **4** at different molar ratios ***r*** = [compound] / [polynucleotide], **pH = 5.0** (left) and **pH=7.0** (right), sodium cacodylate buffer, I = 0.05 mol dm^{-3}.

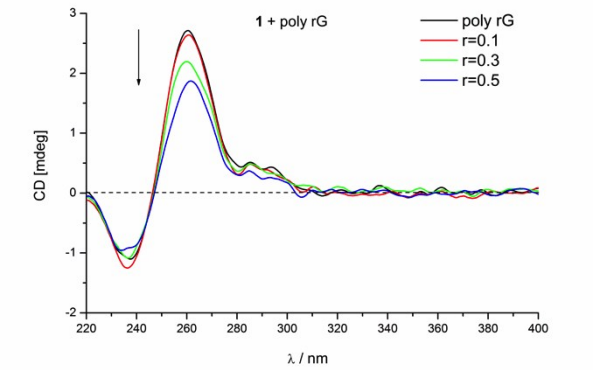

Figure S39. Changes in the CD spectrum of poly rG (c = 2.0 × 10^{-5} mol dm^{-3}) upon addition of **1** at different molar ratios ***r*** = [compound] / [polynucleotide], **pH=7.0**, sodium cacodylate buffer, I = 0.05 mol dm^{-3}.

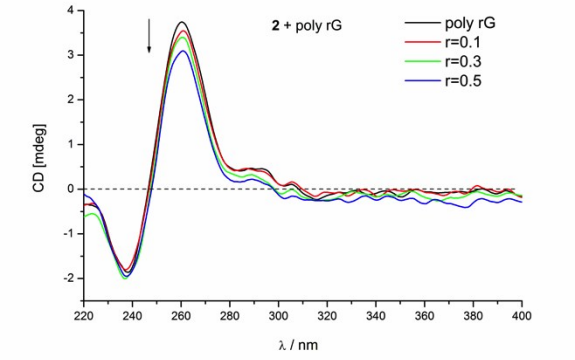

Figure S40. Changes in the CD spectrum of poly rG (c = 2.0 × 10^{-5} mol dm^{-3}) upon addition of **2** at different molar ratios ***r*** = [compound] / [polynucleotide], **pH=7.0**, sodium cacodylate buffer, I = 0.05 mol dm^{-3}.

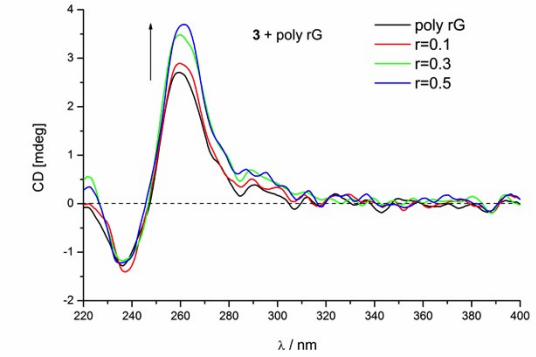

Figure S41. Changes in the CD spectrum of poly rG (c = 2.0 × 10^{-5} mol dm^{-3}) upon addition of **3** at different molar ratios ***r*** = [compound] / [polynucleotide], **pH=7.0**, sodium cacodylate buffer, I = 0.05 mol dm^{-3}.

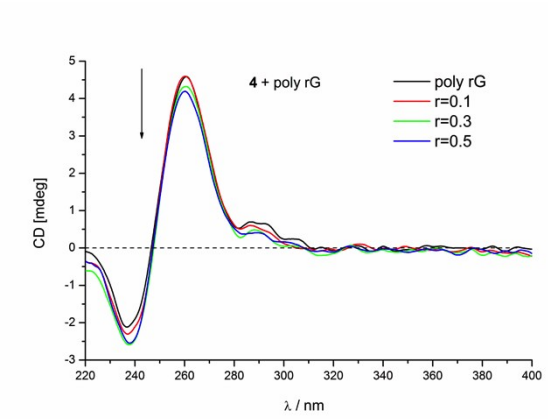

Figure S42. Changes in the CD spectrum of poly rG (c = 2.0 × 10^{-5} mol dm^{-3}) upon addition of **4** at different molar ratios ***r*** = [compound] / [polynucleotide], **pH=7.0**, sodium cacodylate buffer, I = 0.05 mol dm^{-3}.

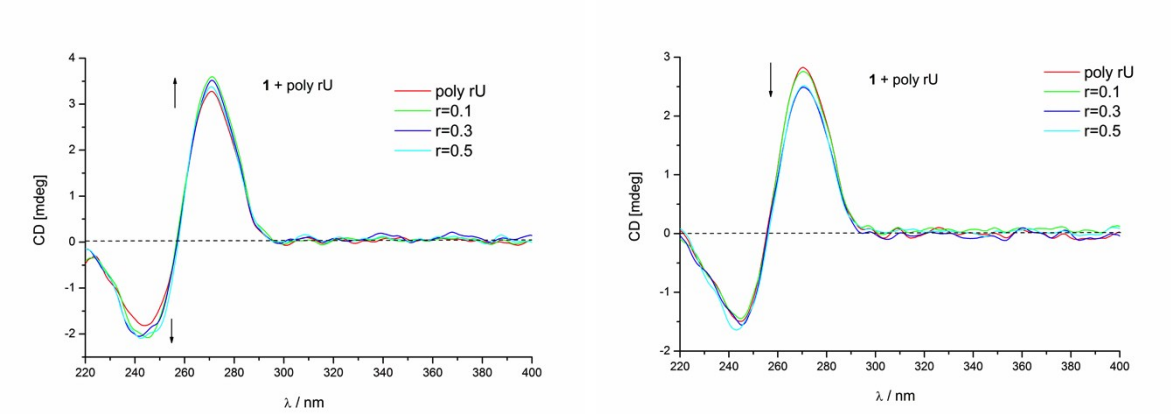

Figure S43. Changes in the CD spectrum of poly rU (c = 2.0 × 10^{-5} mol dm^{-3}) upon addition of **1** at different molar ratios ***r*** = [compound] / [polynucleotide], **pH = 5.0** (left) and **pH=7.0** (right), sodium cacodylate buffer, I = 0.05 mol dm^{-3}.

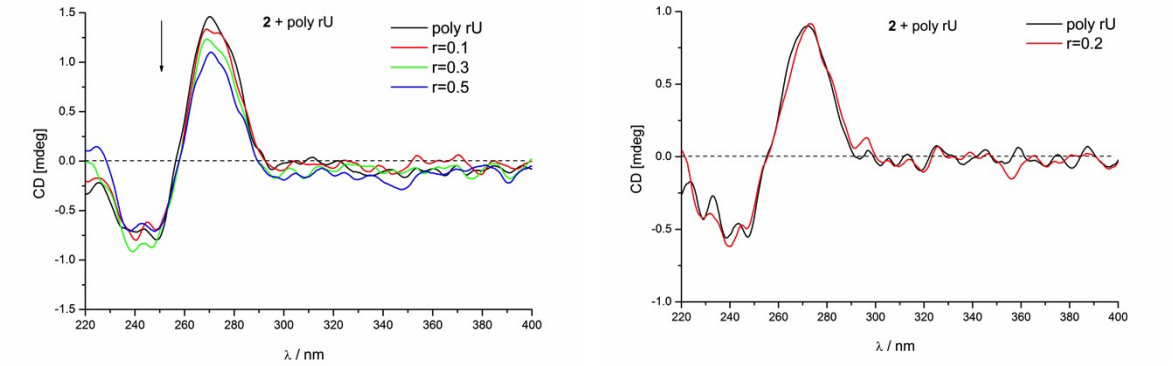

Figure S44. Changes in the CD spectrum of poly rU (c = 2.0 × 10^{-5} mol dm^{-3}) upon addition of **2** at different molar ratios ***r*** = [compound] / [polynucleotide], **pH = 5.0** (left) and **pH=7.0** (right), sodium cacodylate buffer, I = 0.05 mol dm^{-3}.

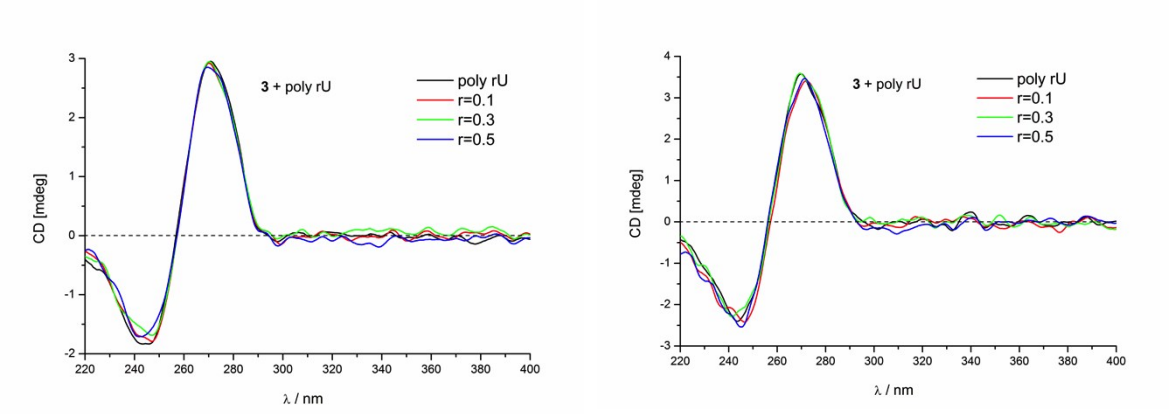

Figure S45. Changes in the CD spectrum of poly rU (c = 2.0 × 10^{-5} mol dm^{-3}) upon addition of **3** at different molar ratios ***r*** = [compound] / [polynucleotide], **pH = 5.0** (left) and **pH=7.0** (right), sodium cacodylate buffer, I = 0.05 mol dm^{-3}.

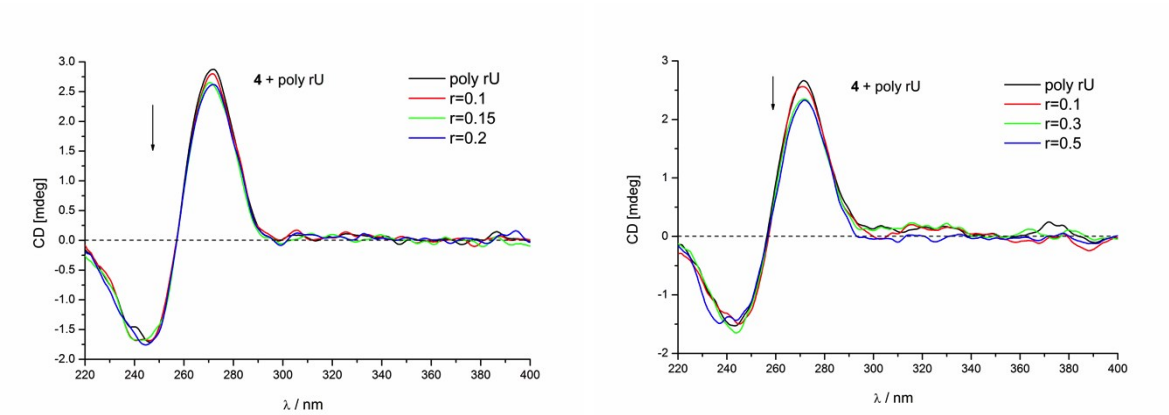

Figure S46. Changes in the CD spectrum of poly rU (c = 2.0 × 10^{-5} mol dm^{-3}) upon addition of **4** at different molar ratios ***r*** = [compound] / [polynucleotide], **pH = 5.0** (left) and **pH=7.0** (right), sodium cacodylate buffer, I = 0.05 mol dm^{-3}.

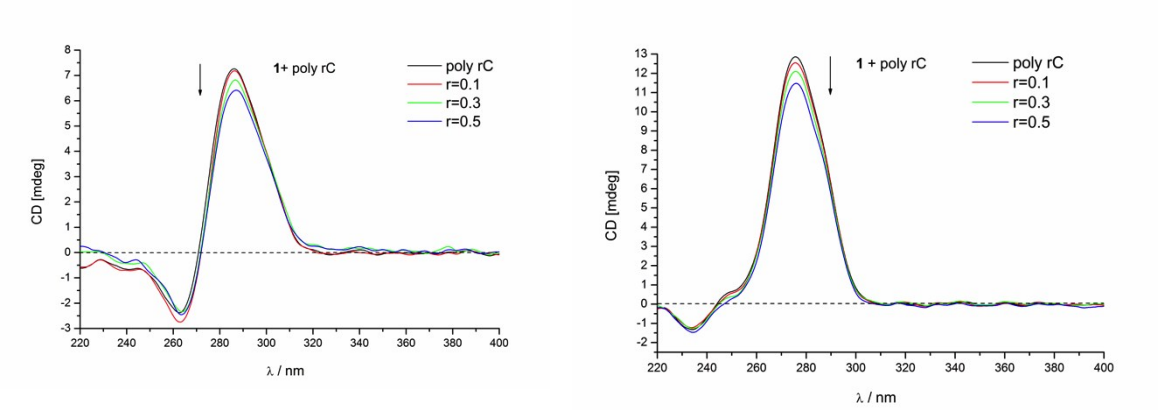

Figure S47. Changes in the CD spectrum of poly rC (c = 2.0 × 10^{-5} mol dm^{-3}) upon addition of **1** at different molar ratios ***r*** = [compound] / [polynucleotide], **pH = 5.0** (left) and **pH=7.0** (right), sodium cacodylate buffer, I = 0.05 mol dm^{-3}.

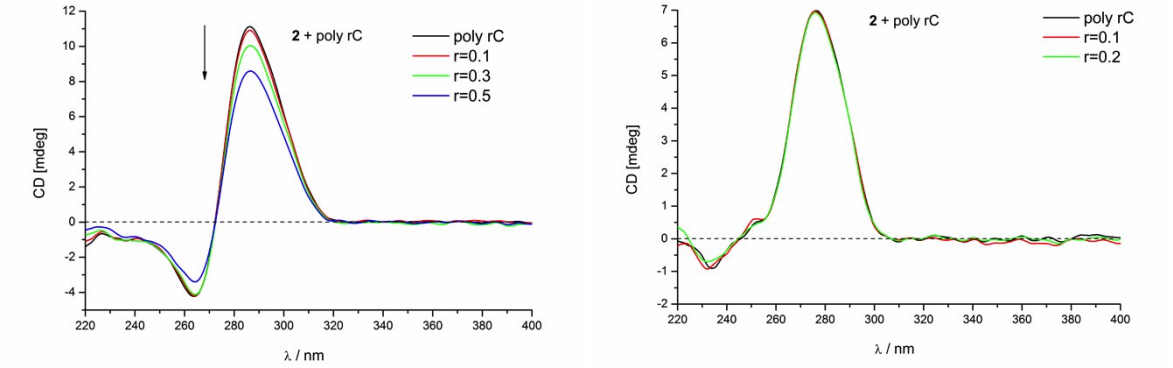

Figure S48. Changes in the CD spectrum of poly rC (c = 2.0 × 10^{-5} mol dm^{-3}) upon addition of **2** at different molar ratios ***r*** = [compound] / [polynucleotide], **pH = 5.0** (left) and **pH=7.0** (right), sodium cacodylate buffer, I = 0.05 mol dm^{-3}.

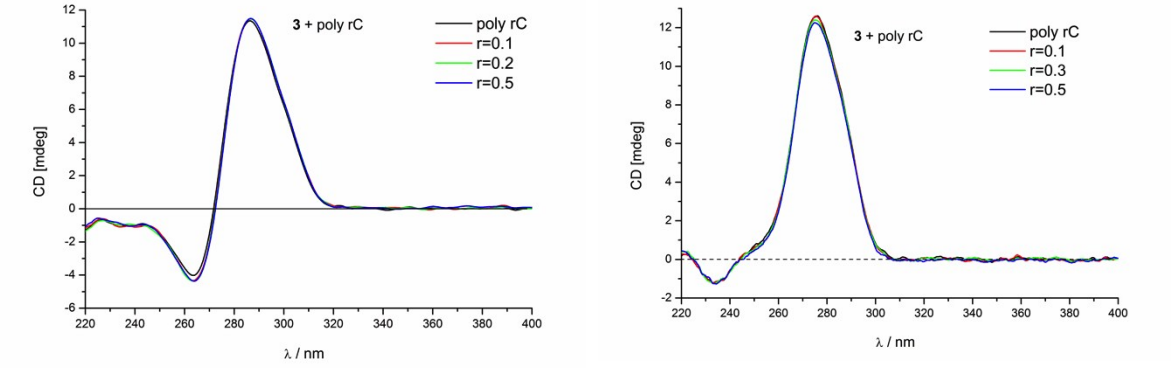

Figure S49. Changes in the CD spectrum of poly rC (c = 2.0 × 10^{-5} mol dm^{-3}) upon addition of **3** at different molar ratios ***r*** = [compound] / [polynucleotide], **pH = 5.0** (left) and **pH=7.0** (right), sodium cacodylate buffer, I = 0.05 mol dm^{-3}.

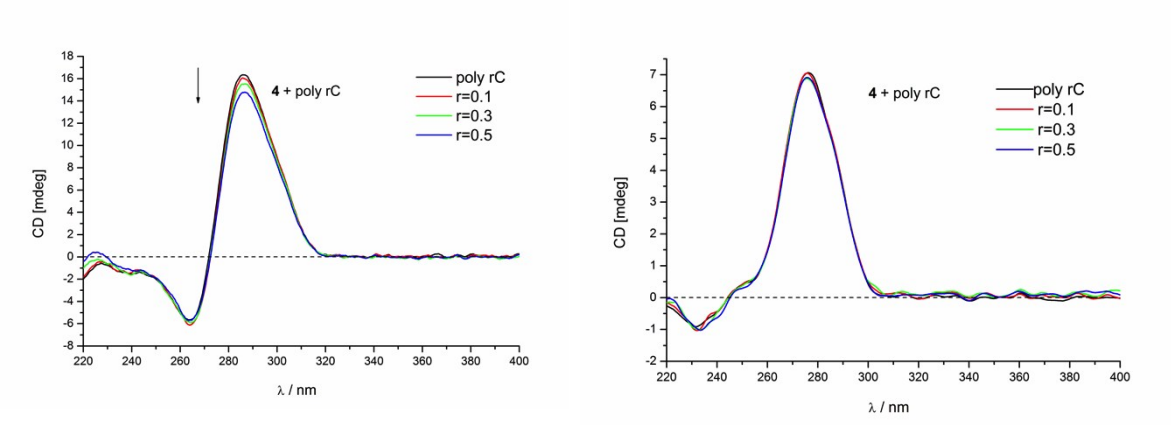

Figure S50. Changes in the CD spectrum of poly rC (c = 2.0 × 10^{-5} mol dm^{-3}) upon addition of **4** at different molar ratios ***r*** = [compound] / [polynucleotide], **pH = 5.0** (left) and **pH=7.0** (right), sodium cacodylate buffer, I = 0.05 mol dm^{-3}.

3.3. Fluorimetric titrations of 1-4 with ds- and ss-polynucleotides

Large errors with Scatchard analysis are often encountered (please see I. R. Klotz, Ligand-Receptor Energetics, John Wiley & Sons, Inc. New York, 1997). Since the concentration of observable species can determine the number of binding sites reflected in the isotherm, the apparent stoichiometry can change based upon the concentration of the observable species. In addition, the errors associated with assigning spectral properties of the 100% "free" versus the 100% "bound" become amplified in all the data points, since the fraction bound at each data point is calculated from these two extremes. The data points for the 100% free and the 100% bound states are, therefore, "weighed" much more heavily than the points in the middle of the titration.

On the other hand, non-linear analysis of binding data can help reduce the errors associated with quantifying the spectral properties of these "extreme" (and often inaccurate) data points. Non-linear analysis typically weighs all data points equally and fits all the points to a theoretical curve. However, it is advisable to carefully choose experimental conditions to assure that all dye molecules bind to dominant binding sites – this is done by preliminary experiment for rough estimation of binding affinity and then repeating more detailed titration at conditions of an excess of DNA/RNA binding sites over c(dye), which allows each dye molecule to find its dominant binding site according

to J.D. Mc Ghee, P.H. von Hippel formalism for non-cooperative binding (ref. 26b in the manuscript). More detailed considerations how to organize titration experiment and analysis are nicely summarised in J. Lah and G. Vesnaver, J Mol Biol, 2004, 342, 73 (pp 80).

According to all mentioned we collected the most of fluorimetric titration data in the range r[dye]/[DNA]=0.1 – 0.01, which also according to thermal denaturation and CD experiments guaranteed that each dye molecule will independently find dominant binding site.

Table S2. Stability constants (log*Ks*)[a] and spectroscopic properties of complexes ΔI [b] of **1-4** with ds-polynucleotides calculated according to fluorimetric titrations (Na-cacodylate buffer, c = 0.05 M, pH = 7.0, λ_{exc}= 305nm, λ_{em}= 330 – 450 nm, c(**1-4**) = 1-2 × 10^{-6} M).

	ct DNA log *Ks*[a]/ΔI[b]	poly rA-poly rU log *Ks*[a] / ΔI[b]
1	4.67 / -62%	4.57/ -43%
2	4.45 /-46%	4.46 /-23%
3	[c]	[c]
4	4.57 / -30%	>4[d] /-15%

[a] Processing of titration data by means of Scatchard equation[3] gave values of ratio n $_{[\text{bound peptide}]\,/\,[\text{polynucleotide}]}$ = 0.15 ± 0.05 for most complexes; for easier comparison values of log Ks are recalculated for fixed n=0.15; correlation coefficients were >0.98-0.99 for all calculated *Ks;* [b] Changes of fluorescence of compound **1-4** induced by complex formation ($\Delta I = (I_{lim} - I_0) \times 100 / I_0$; where I_0 is calculated emission intensity of free compound and I_{lim} is emission intensity of a complex calculated by processing the titration data with the Scatchard); [c] small and linear fluorescence change / no fluorescence change disabled calculation of stability constant; [d] Small total emission change and/or high divergences of fluorescence intensities disabled accurate calculation of stability constant / enabled only estimation of stability constant.

Table S3. Stability constants (logK_s)[a] and spectroscopic properties of complexes ΔI [b] of **1-4** with ss-polynucleotides calculated according to fluorimetric titrations (Na-cacodylate buffer, c = 0.05 M, pH = 7.0 λ_{exc}= 305nm, λ_{em}= 330 - 450, c(**1-4**) = 2 × 10^{-6} M).

	poly rA log *Ks*[a]/ΔI[b]	poly rG log *Ks*[a] / ΔI[b]	poly rU log *Ks*[a] / ΔI[b]	poly rC log *Ks*[a] / ΔI[b]
1	>6[c] / -12%	6.15 / -58%	6.26 / -26%	6.11 / -17%
2	>6 [c] / -5%	5.82 / -45%	>6[c] / -13%	>6[c] /-15%
3	[d]	[d]	[d]	[d]
4	5-6 [c] / -10%	5.74 / -47%	5-6[c] / -18%	5-6[c] / -11%

[a] Processing of titration data by means of Scatchard equation2 gave values of ratio n $_{[bound\ peptide]\ /\ [polynucleotide]}$ = 0.15 ± 0.05 for most complexes; for easier comparison values of log Ks are recalculated for fixed n=0.15; correlation coefficients were >0.98-0.99 for all calculated *Ks;* [b] Changes of fluorescence of compound **1-4** induced by complex formation ($\Delta I = (I_{lim} - I_0) \times 100 / I_0$; where I_0 is calculated emission intensity of free compound and I_{lim} is emission intensity of a complex calculated by processing the titration data with the Scatchard equation); [c] Small total emission change and/or high divergences of fluorescence intensities allowed only estimation of Ks; [d] small and linear fluorescence change / no fluorescence change hampered calculation Ks.

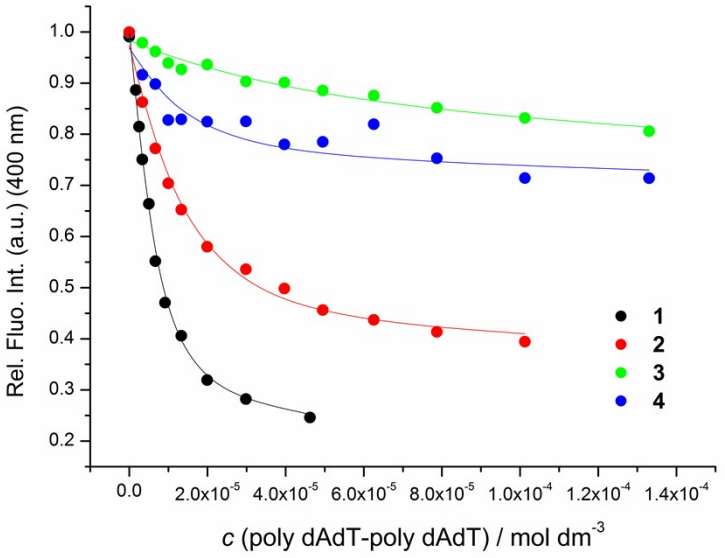

Figure S51. Experimental (•) and calculated (–) (by Scatchard eq., Table 1) fluorescence intensities of compounds **1-4** upon addition of poly dAdT-poly dAdT; values were normalized for easier comparison. Na-cacodylate buffer, **pH 5.0**, *I*= 0.05 M, λ_{exc} = 310 nm.

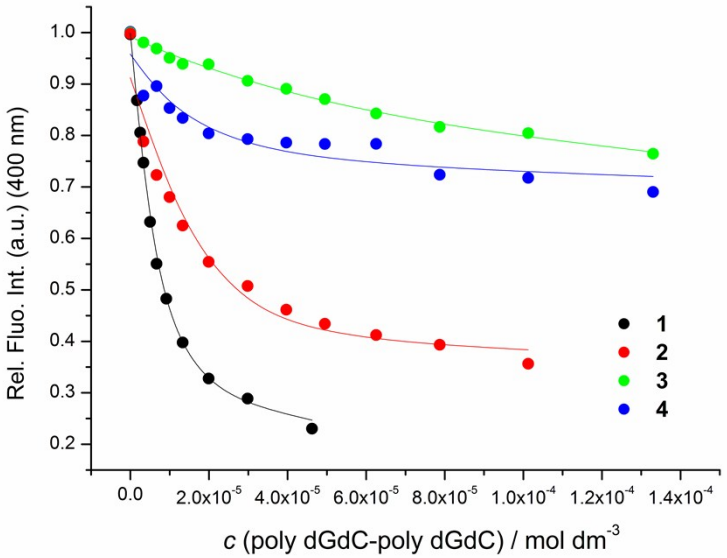

Figure S52. Experimental (•) and calculated (–) (by Scatchard eq., Table 1) fluorescence intensities of compounds **1-4** upon addition of poly dGdC-poly dGdC; values were normalized for easier comparison. Na-cacodylate buffer, **pH 5.0**, *I*= 0.05 M, λ_{exc} = 310 nm.

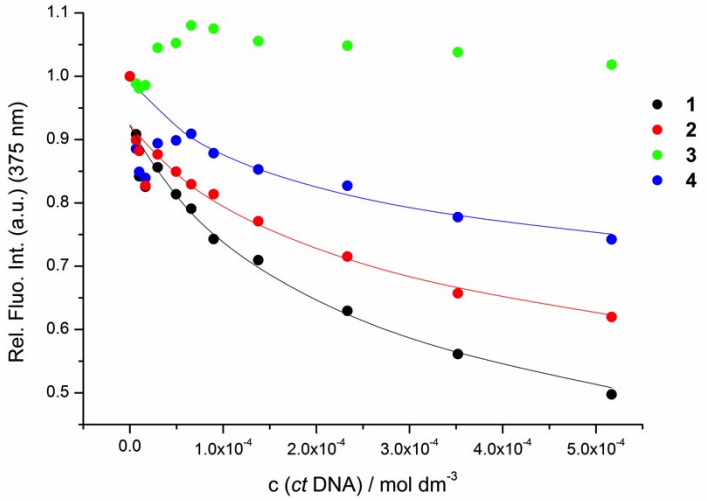

Figure S53. Experimental (•) and calculated (–) (by Scatchard eq., Table S2) fluorescence intensities of compounds **1-4** upon addition of ct DNA; values were normalized for easier comparison. Na-cacodylate buffer, **pH 7.0**, *I*= 0.05 M, λ_{exc} = 305 nm.

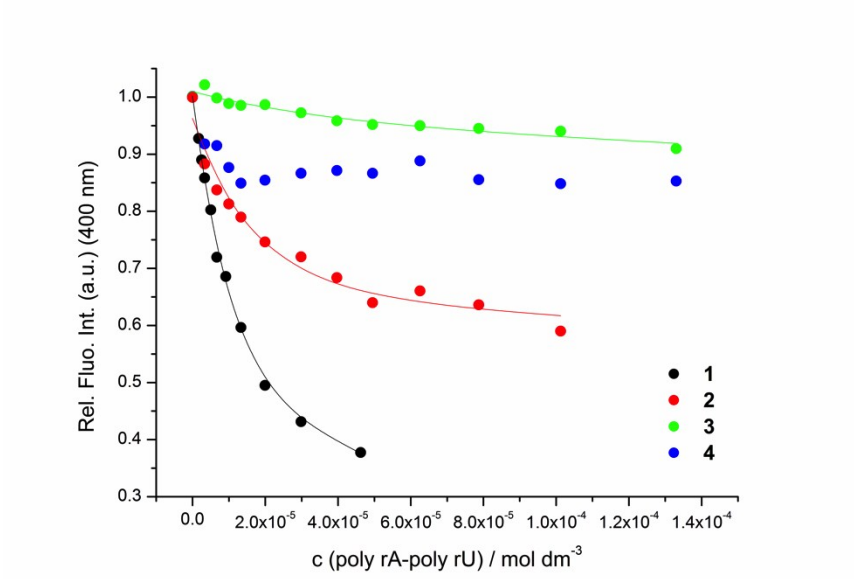

Figure S54. Experimental (•) and calculated (–) (by Scatchard eq., Table 1) fluorescence intensities of compounds **1-4** upon addition of poly rA-poly rU; values were normalized for easier comparison. Na-cacodylate buffer, **pH 5.0**, *I*= 0.05 M, λ_{exc} = 310 nm.

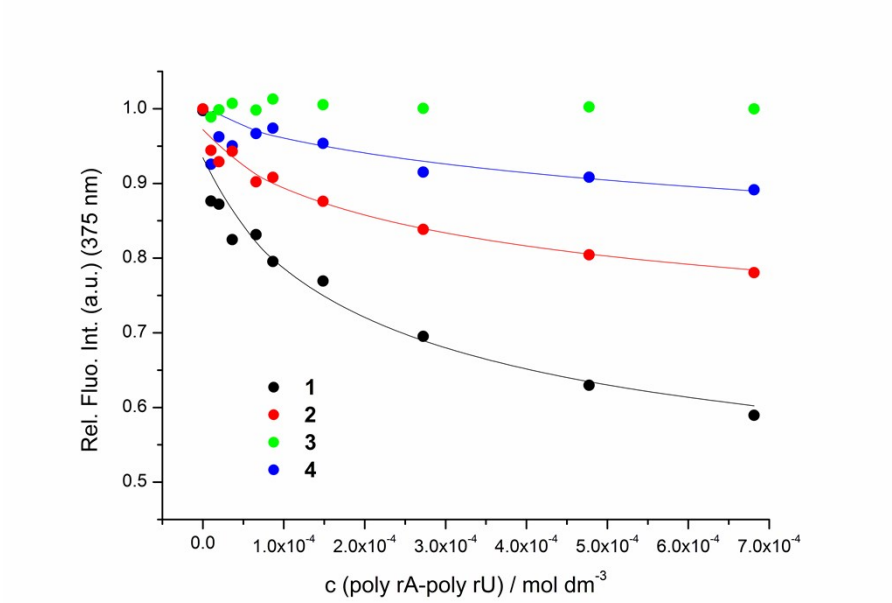

Figure S55. Experimental (•) and calculated (–) (by Scatchard eq., Table S2) fluorescence intensities of compounds **1-4** upon addition of poly rA-poly rU; values were normalized for easier comparison. Na-cacodylate buffer, **pH 7.0**, *I*= 0.05 M, λ_{exc} = 305 nm.

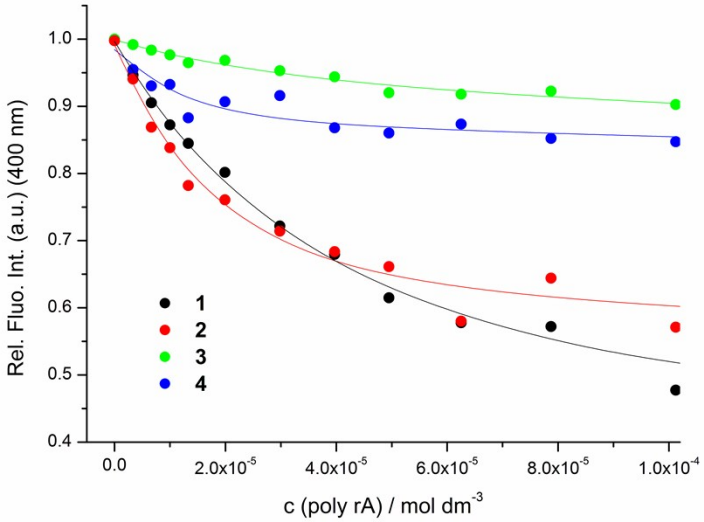

Figure S56. Experimental (•) and calculated (–) (by Scatchard eq., Table 2) fluorescence intensities of compounds **1-4** upon addition of poly rA; values were normalized for easier comparison. Na-cacodylate buffer, **pH 5.0**, *I*= 0.05 M, λ_{exc} = 310 nm.

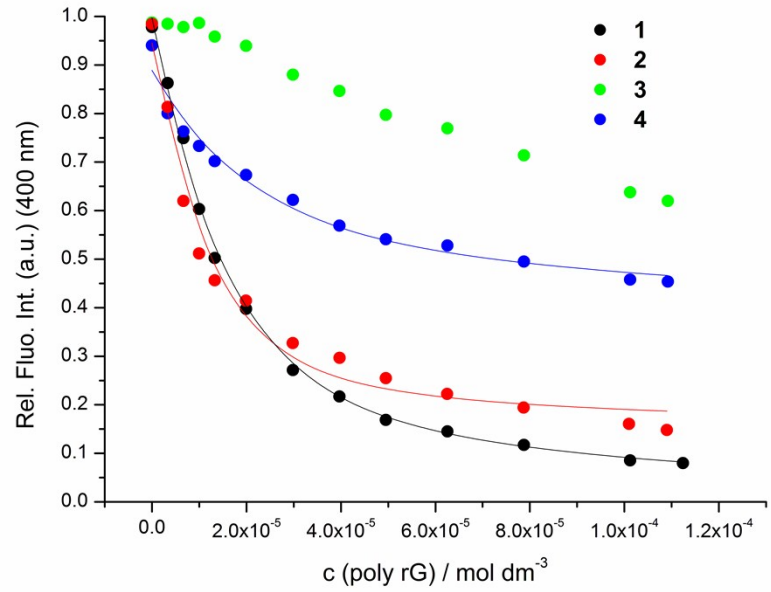

Figure S57. Experimental (•) and calculated (–) (by Scatchard eq., Table 2) fluorescence intensities of compounds **1-4** upon addition of poly rG; values were normalized for easier comparison. Na-cacodylate buffer, **pH 5.0**, *I*= 0.05 M, λ_{exc} = 310 nm.

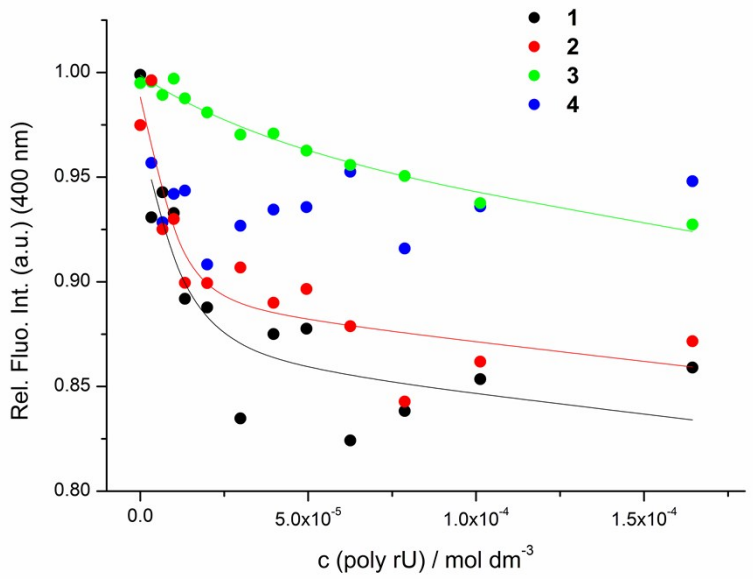

Figure S58. Experimental (•) and calculated (–) (by Scatchard eq., Table 2) fluorescence intensities of compounds **1-4** upon addition of poly rU; values were normalized for easier comparison. Na-cacodylate buffer, **pH 5.0**, *I*= 0.05 M, λ_{exc} = 310 nm.

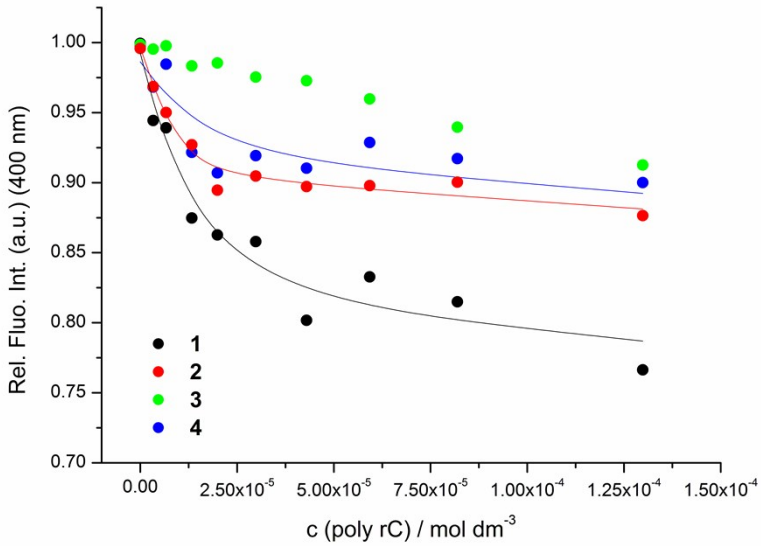

Figure S59. Experimental (•) and calculated (–) (by Scatchard eq., Table 2) fluorescence intensities of compounds **1-4** upon addition of poly rC; values were normalized for easier comparison. Na-cacodylate buffer, **pH 5.0**, *I*= 0.05 M, λ_{exc} = 310 nm.

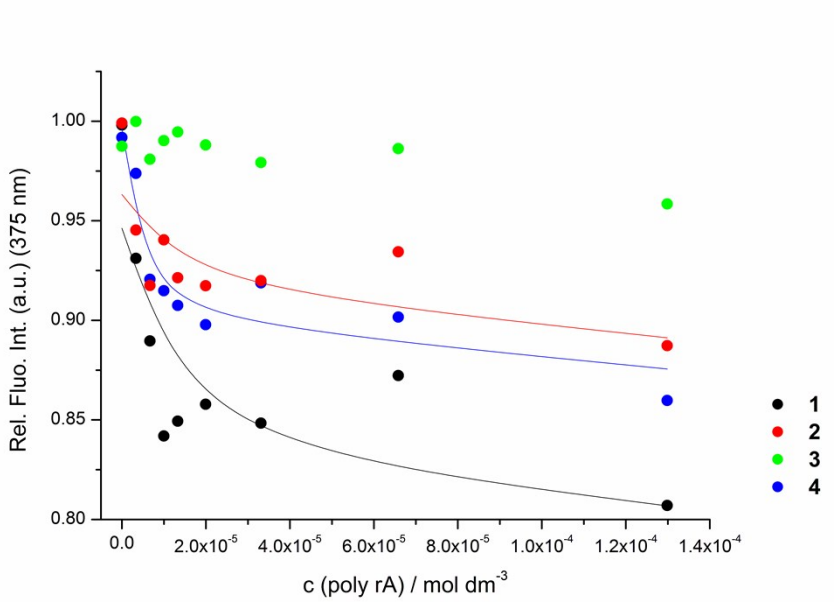

Figure S60. Experimental (•) and calculated (–) (by Scatchard eq., Table S3) fluorescence intensities of compounds **1-4** upon addition of poly rA; values were normalized for easier comparison. Na-cacodylate buffer, **pH 7.0**, *I*= 0.05 M, λ_{exc} = 305 nm.

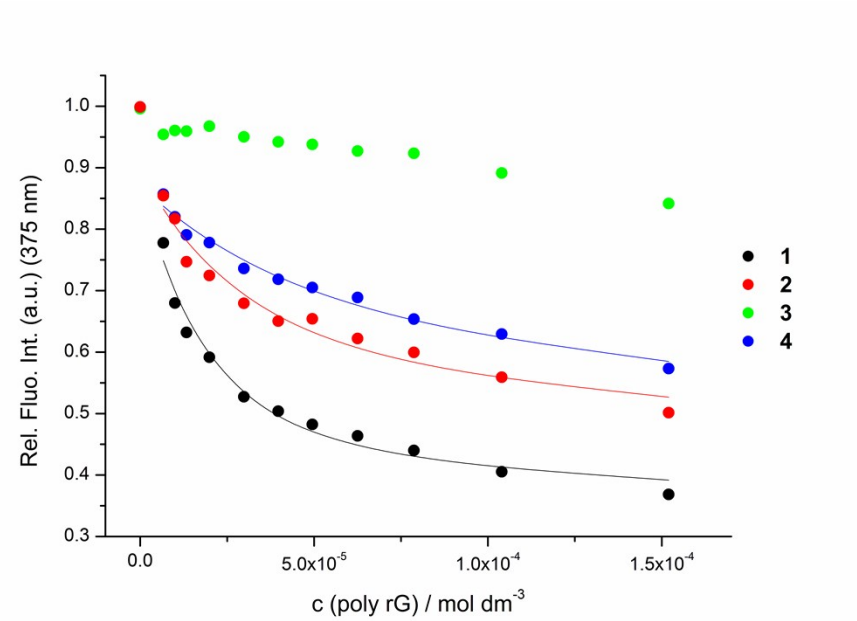

Figure S61. Experimental (•) and calculated (–) (by Scatchard eq., Table S3) fluorescence intensities of compounds **1-4** upon addition of poly rG; values were normalized for easier comparison. Na-cacodylate buffer, **pH 7.0**, *I*= 0.05 M, λ_{exc} = 305 nm.

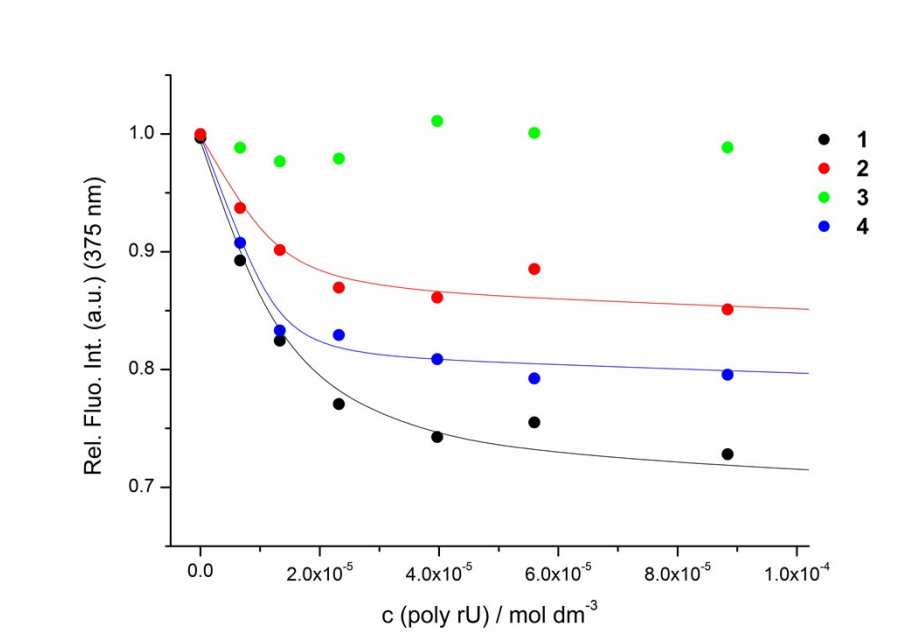

Figure S62. Experimental (•) and calculated (–) (by Scatchard eq., Table S3) fluorescence intensities of compounds **1-4** upon addition of poly rU; values were normalized for easier comparison. Na-cacodylate buffer, **pH 7.0**, *I*= 0.05 M, λ_{exc} = 305 nm.

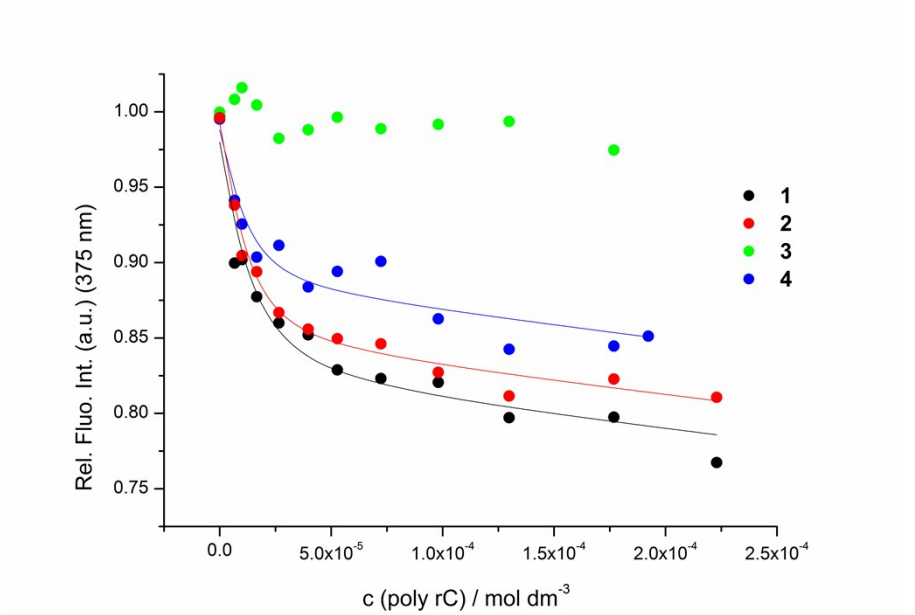

Figure S63. Experimental (•) and calculated (–) (by Scatchard eq., Table S3) fluorescence intensities of compounds **1-4** upon addition of poly rC; values were normalized for easier comparison. Na-cacodylate buffer, **pH 7.0**, *I*= 0.05 M, λ_{exc} = 305 nm.

4. Biology

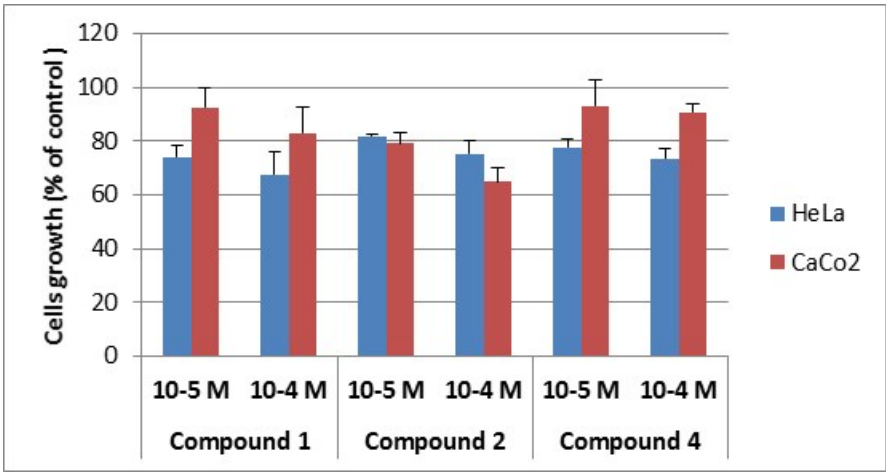

Figure S64. Dose-response profiles for compounds **1**, **2** and **4** tested in vitro on a human tumour cell lines HeLa, CaCo2, and K562 and normal epithelial cells (MDCK1). Data represents mean values ± standard deviation (SD) of three independent experiments. Exponentially growing cells were treated during 72-hrs period. Cytotoxicity was analysed using MTT survival assay.

5. Molecular modelling

Construction of schematic presentation on Figure 3:

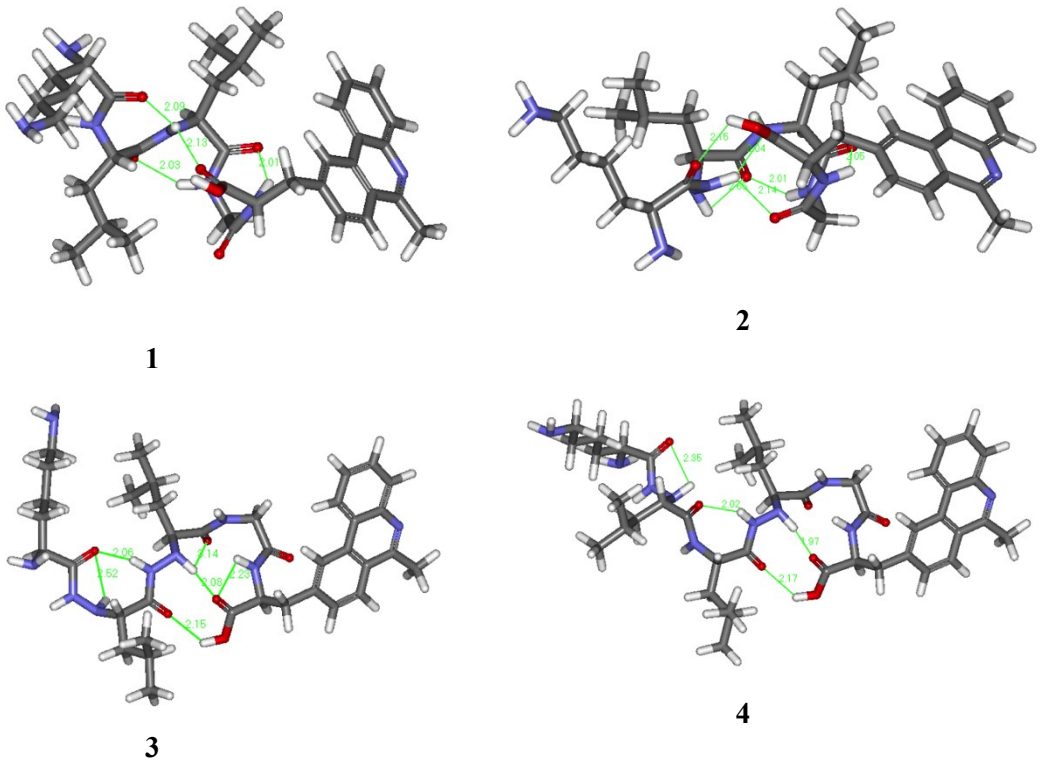

1 **2** **3** **4**

Figure S65. 1-4 were submitted to MM2 calculations by a modified version of Allinger's MM2 force field, integrated into the ChemBio3D 11.0 programme, whereby obtained structures demonstrate the possible intramolecular H-bond network for each peptide, and resulting secondary structure.

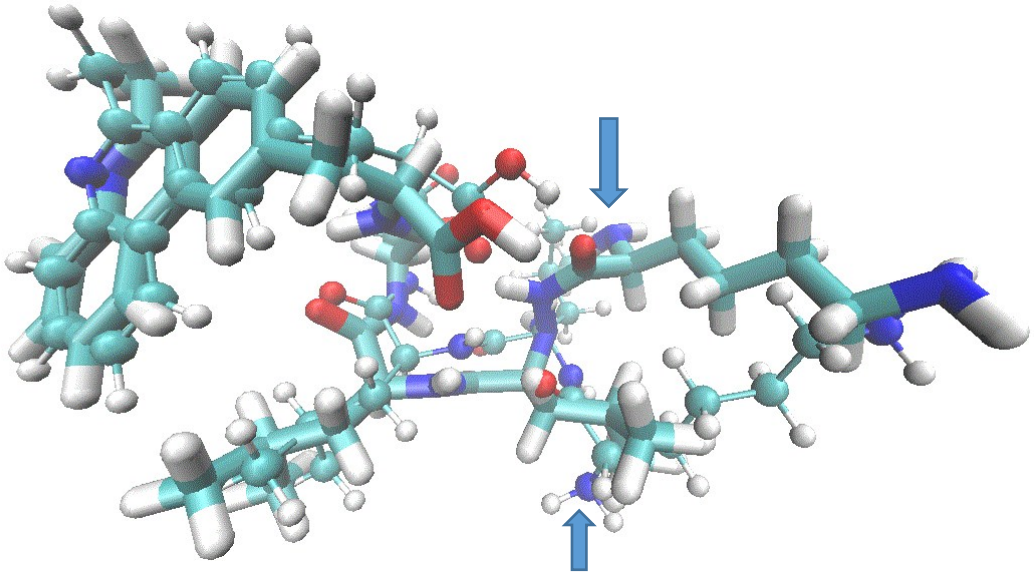

Figure S66. Overlap of models: **1** (rod), **2** (stick-and-ball), arrows show peptide N-terminus.

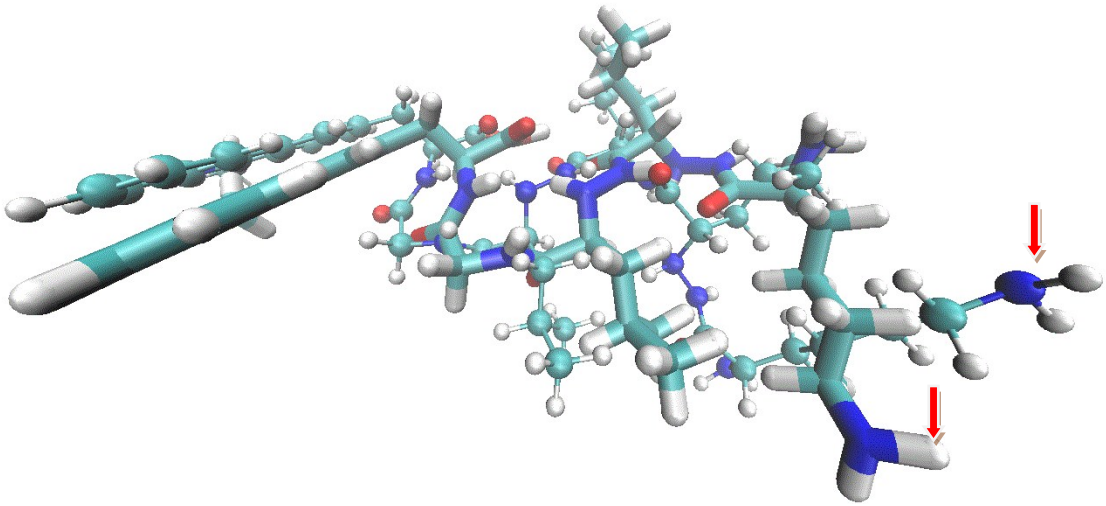

Figure S67. Overlap of models: **3** (rod), **4** (stick-and-ball), note different orientation of Lys-side chains (arrow marked).

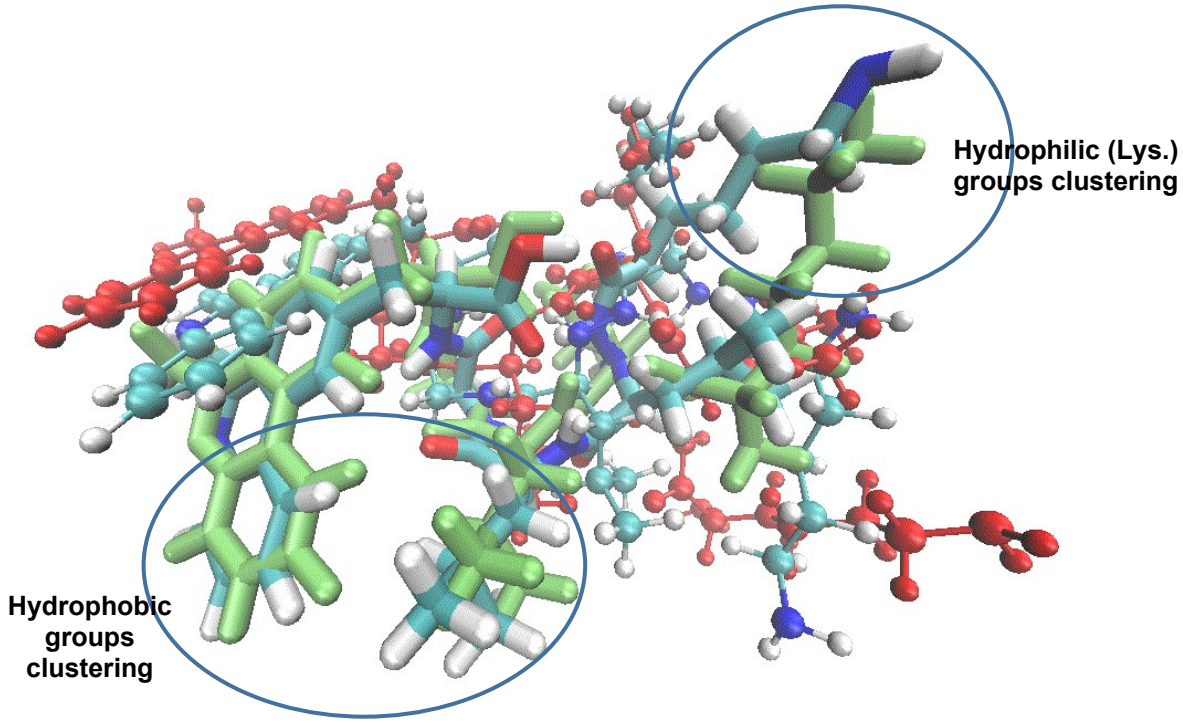

Figure S68. **1 (rod, blue/white); 2 (rod, green); 3 (stick-and-ball, blue/white); 4 (stick-and-ball, red)**

DISCUSSION:

In general, we saw two pairs of molecules, which models overlap significantly.

- Models of **1**, **2** overlap well, only difference is position of peptide N-terminus (see arrows in Fig. S50)
- Models of **3**, **4** overlap well (Fig. S51), only difference is somewhat different orientation of Lys. Side chains but due to flexibility it might be considered similar

However, in **1-4** overlap (Fig. S52) there are two major differences: only **1**, **2** show hydrophobic groups clustering (AlaP with hLeu), and simultaneously positively charged Lys chains) are oriented oppositely to hydrophobic groups. Structures of **3** and **4** are longitudinally stretched, whereby central set of highly hydrophobic hLeu groups forms very voluminous barrel-like central structure, while AlaP and Lys chain sticking out at the ends.

---

[1] C. R. Cantor, P. R. Schimmel, *Biophysical Chemistry,* vol. 3,. WH Freeman and Co., San Francisco, 1980, 1109-1181.

[2] Rodger A., Norden B., In *Circular Dichroism and Linear Dichroism*; Oxford University Press: New York, 1997, Chapter 2.

[3] a) J. D. Mc Ghee and P. H. von Hippel, J. Mol. Biol., 1974, 86, 469–489; b) G. Scatchard, Ann. N.Y. Acad. Sci., 1949, 51, 660–672